

AGONIST-MODULATED REGULATION OF AMP-ACTIVATED PROTEIN KINASE IN ENDOTHELIAL CELLS: EVIDENCE FOR AN AMPK→RAC1→AKT→eNOS PATHWAY*

Yehoshua C. Levine¹, Gordon K. Li¹, and Thomas Michel¹

From the Cardiovascular Division¹, Brigham and Women's Hospital,
Harvard Medical School, Boston, Massachusetts 02115

Address correspondence to: Thomas Michel, MD PhD, Cardiovascular Division,
Brigham and Women's Hospital, 75 Francis Street, Boston, MA 02115. Tel.: 617-732-
7376; Fax: 617-732-5132; E-mail: tmichel@research.bwh.harvard.edu.

The endothelial isoform of nitric oxide synthase (eNOS), a key determinant of vascular homeostasis, is a calcium/calmodulin-dependent phosphoprotein regulated by diverse cell surface receptors. Vascular endothelial growth factor (VEGF) and sphingosine 1-phosphate (S1P) stimulate eNOS activity through Akt/PI3K and calcium-dependent pathways. AMP-activated protein kinase (AMPK) also activates eNOS in endothelial cells; however, the molecular mechanisms linking agonist-mediated AMPK regulation with eNOS activation remain incompletely understood. We studied the role of AMPK in VEGF- and S1P-mediated eNOS activation and found that both agonists lead to a striking increase in AMPK phosphorylation in pathways involving the calcium/calmodulin-dependent protein kinase kinase β (CaMKK β). Treatment with tyrosine kinase inhibitors or the PI3K inhibitor wortmannin demonstrated differential effects of VEGF versus S1P. siRNA-mediated knockdown of AMPK α 1 or Akt1 impairs the stimulatory effects of both VEGF and S1P on eNOS activation. AMPK α 1 knockdown impaired agonist-mediated Akt phosphorylation, whereas Akt1 knockdown did not affect AMPK activation, thus suggesting that AMPK lies upstream of Akt in the pathway leading from receptor activation to eNOS stimulation. Importantly, we found that siRNA-mediated knockdown of AMPK α 1

abrogates agonist-mediated activation of the small GTPase Rac1. Conversely, siRNA-mediated knockdown of Rac1 decreased the agonist-mediated phosphorylation of AMPK substrates without affecting that of AMPK, implicating Rac1 as a molecular link between AMPK and Akt in agonist-mediated eNOS activation. Finally, siRNA-mediated knockdown of caveolin-1 significantly enhanced AMPK phosphorylation, suggesting that AMPK is negatively regulated by caveolin-1. Taken together, these results suggest that VEGF and S1P differentially regulate AMPK, and establish a central role for an agonist-modulated AMPK→Rac1→Akt axis in the control of eNOS in endothelial cells.

The AMP-activated protein kinase (AMPK) is an evolutionarily conserved serine/threonine heterotrimeric kinase that was initially characterized as a "fuel gauge" modulating cellular energy flux in eukaryotic cells in response to changes in intracellular AMP levels (for review, see Ref. 1). More recent studies have identified a broader role for AMPK in cellular homeostasis and signaling: AMPK is now known to be regulated by a family of upstream AMPK kinases, including the calcium/calmodulin-dependent protein kinase kinase β (CaMKK β) (2, 3) and the tumor suppressor kinase LKB1 (4). After AMPK undergoes phosphorylation at the threonine 172 site in the activation loop

of its catalytic α -subunit, the kinase is activated (1) and can mediate numerous energy-conserving cellular processes, such as promotion of glucose uptake and glycolysis (5), acceleration of mitochondrial biogenesis (6), and stimulation of fatty acid oxidation with concomitant inhibition of fatty acid synthesis via phosphorylation and inactivation of acetyl-CoA carboxylase (ACC) (7). In addition to phosphorylating ACC, AMPK also has been shown to phosphorylate the endothelial isoform of nitric oxide synthase (eNOS) on serine 1179 in endothelial cells and cardiac myocytes (8). AMPK appears to be involved in the pathways of eNOS activation evoked by a variety of extracellular stimuli that modulate eNOS in endothelial cells, including metformin (9), adiponectin (10, 11), hypoxia (12), and HMG CoA reductase inhibitors (13). The activation of eNOS by AMPK has been implicated in many of the bioenergetic (14), angiogenic (12), and anti-inflammatory effects of AMPK in endothelial cells.

Despite the accumulating evidence linking AMPK with eNOS in the vascular endothelium, the molecular pathways involved in AMPK-mediated eNOS activation remain incompletely characterized. eNOS is also activated by the protein kinase Akt, a phosphoinositide 3-kinase (PI3K)-dependent effector that plays critical roles in numerous cellular responses including angiogenesis and endothelial cell survival (15). A number of recent reports have studied both AMPK and Akt in the context of eNOS activation or nitric oxide release, but the relative role of these protein kinases remains controversial, with evidence for (16) and against (17) an AMPK/Akt interaction upstream of eNOS.

In addition to the uncertain relationship between AMPK and Akt, the eNOS-activating agonists that lead to AMPK phosphorylation are incompletely characterized, as are the pathways that connect these different phosphorylation pathways to eNOS activation and endothelial functional responses including migration and tube formation. It remains unclear whether

vascular endothelial growth factor (VEGF), an angiogenic polypeptide growth factor and potent eNOS agonist, promotes AMPK phosphorylation under normoxic conditions (12), and a recent study (18) that implicated AMPK in VEGF-mediated eNOS activation did not define the mechanisms involved in this response. Akt and eNOS are also potentially activated by the platelet-derived lipid mediator sphingosine 1-phosphate (S1P) (19), but the phosphorylation of AMPK by S1P and the possible involvement of AMPK in S1P-mediated eNOS activation and cell motility have not been previously described. Both VEGF and S1P act in part by stimulating an influx of calcium into the endothelium (19, 20), thereby providing a route for AMPK activation that may depend upon CaMKK. The differential phosphorylation of AMPK by both VEGF and S1P therefore represents a plausible mechanism of eNOS regulation in endothelial cells.

Caveolae are plasmalemmal microdomains originally identified on the surface of endothelial and epithelial cells (21). The scaffolding/regulatory protein of caveolae, caveolin-1 (22, 23), is known to interact with and modulate the function of eNOS in endothelial cells (24). We have demonstrated that caveolin-1 negatively regulates the small GTPase Rac1 (25, 26), which in turn modulates the PI3K/Akt/eNOS pathway and regulates migration in endothelial cells (24, 27). It is therefore possible that AMPK regulates agonist-mediated eNOS activation and endothelial migration by interacting with caveolin-1 or Rac1 in endothelial cells.

In the present study, we provide evidence that the eNOS agonists VEGF and S1P differentially promote the phosphorylation of AMPK in vascular endothelial cells in distinct receptor-modulated pathways that involve tyrosine kinases and caveolin-1. Using pharmacological approaches as well as siRNA-mediated protein knockdown methodologies, we elucidate the molecular mechanisms of eNOS activation downstream of AMPK, and identify a novel AMPK-Rac1-Akt pathway that functions as a critical

determinant of eNOS activity as well as endothelial cell migration and tube formation in the vascular endothelium.

EXPERIMENTAL PROCEDURES

Materials - Fetal bovine serum (FBS) was purchased from Hyclone (Logan, CT); all other cell culture reagents, media, and Lipofectamine 2000 transfection reagent were from Invitrogen. SIP and PP2 were from BioMol (Plymouth Meeting, PA). VEGF, genistein, wortmannin, cyclosporine, SB203580, STO-609, and Compound C were from Calbiochem. Polyclonal antibodies directed against phospho-AMPK (thr172), AMPK, phospho-ACC (ser79), ACC, phospho-eNOS (ser1179), phospho-Akt (ser473), Akt, phospho-GSK3 β (ser9), phospho-ERK1/2 (thr202/tyr204), and ERK1/2 were from Cell Signaling Technologies (Beverly, MA). Polyclonal Akt1 antibody was from Chemicon. eNOS monoclonal antibody, glycogen synthase kinase-3- β (GSK3- β) monoclonal antibody, and polyclonal caveolin-1 antibody were from BD Transduction Laboratories (Lexington, KY). The monoclonal antibody for VEGFR2 and polyclonal antibody specific for the β isoform of CaMKK were from Santa Cruz Biotechnology (Santa Cruz, CA). Rac1 monoclonal antibody and Rac activation assay kit were from Upstate Biotechnology (Temecula, CA). Super Signal substrate for chemiluminescence detection and secondary antibodies conjugated with horseradish peroxidase were from Pierce. Tris-buffered saline and phosphate-buffered saline (PBS) were from Boston Bioproducts (Ashland, MA). Other reagents were from Sigma.

Cell Culture - Bovine aortic endothelial cells (BAEC) were obtained from Cell Systems (Kirkland, WA) and maintained in culture in Dulbecco's modified Eagle's medium (DMEM) supplemented with FBS (10%, v/v) as described previously (19). Cells were plated onto 0.2% gelatin-coated culture dishes and studied prior to cell confluence between passages 5 and 9.

siRNA Design and Transfection - Our siRNA duplexes were designed on the basis of

established characteristics of siRNA targeting constructs (28). All experimental oligonucleotides were purchased from Ambion (Austin, TX). We designed an AMPK α 1 siRNA corresponding to bases 234-252 from the open reading frame of bovine AMPK α 1: 5'-CCU CAA GCU UUU CAG GCA UdTdT-3' (Ensembl Transcript ID: ENSBTAT00000000016). We also designed an Akt1 siRNA corresponding to bases 1325-1343 from the open reading frame of bovine Akt1 (5'-GGA CGU GUA CGA GAA GAA GdTdT-3'; Ensembl Transcript ID: ENSBTAG00000017636); a CaMKK β siRNA from bases 585-603 of the open reading frame of bovine CaMKK β (5'-GGU GCU GUC CAA AAA GAA AdTdT-3'; Ensembl Transcript ID: ENSBTAG00000010815); and an eNOS siRNA from bases 3948-3966 of the open reading frame of bovine eNOS (5'-CCU GAU CUC UAA AUC AUU CdTdT-3'; Ensembl Transcript ID: ENSBTAT00000007246). siRNA constructs targeting VEGFR2 (32), Rac1 (27), and caveolin-1 (24) have been described previously. A nonspecific control siRNA from Dharmacon (Lafayette, CO) was used as a negative control (5'-AUU GUA UGC GAU CGC AGA CdTdT-3'). BAEC were transfected with siRNA as described previously (24) and analyzed 48 h after transfection.

Drug Treatment and Immunoblotting - 12-16 hours prior to cell treatments, culture medium was changed to serum-free medium. VEGF and SIP were prepared as previously reported (24). Genistein, PP2, CsA, SB203580, wortmannin, STO-609, and Compound C were solubilized in dimethyl sulfoxide and kept at -20 °C; where indicated, dimethyl sulfoxide 0.1% (v/v) was used as the vehicle control. After drug treatments, BAEC were washed with PBS and incubated on ice for 20 min in lysis buffer (50 mM Tris-HCl, pH 7.4, 150 mM NaCl, 1% Nonidet P-40, 0.25% sodium deoxycholate, 1 mM EDTA, 2 mM Na₃VO₄, 1 mM NaF, 2 μ g/ml leupeptin, 2 μ g/ml antipain, 2 μ g/ml soybean trypsin inhibitor, and 2 μ g/ml lima trypsin inhibitor). Cells were harvested by scraping, and then centrifuged for 5 min at 4°C. For immunoblot

analyses, 20 μg of cellular protein was resolved by SDS-PAGE, transferred to nitrocellulose membranes, and probed with antibodies using protocols provided by the suppliers. Densitometric analyses of the Western blots were performed using a ChemiImager 4000 (Alpha-Innotech). When indicated, for the experiments showing densitometry of Western blots, the ordinate is in arbitrary units (a.u.).

NOS activity assay - eNOS activity was quantified as the formation of L-[^3H] citrulline from L-[^3H] arginine in cultured BAEC as described previously in detail (19, 29). Briefly, reactions were initiated by adding L-[^3H] arginine (10 $\mu\text{Ci}/\text{mL}$) plus VEGF or S1P as described below. Each treatment was performed in duplicate cultures, which were then each analyzed in duplicate. The flow-through fraction was analyzed by liquid scintillation counting, and NOS activity was quantitated based on L-[^3H]citrulline formation in the cells; the values were expressed as fmol of L-[^3H]citrulline produced/well/min.

Rac1 Activity Assay - Transfected BAEC in 100-mm dishes were stimulated with VEGF or S1P, and cells were then washed with ice-cold TBS and lysed in lysis buffer (25 mM HEPES, 150 mM NaCl, 1% Nonidet P-40, 10 mM MgCl_2 , 1 mM EDTA, 10% glycerol, 2 mM Na_3VO_4 , 1 mM NaF). Pull-down of GTP-bound Rac was performed by incubating the cell lysates with GST fusion protein corresponding to the p21-binding domain of PAK-1 bound to glutathione-agarose (Upstate Biotechnology) for 1 h at 4°C following instructions provided by the suppliers. The beads were washed three times for 10 min each with lysis buffer, and the protein bound to the beads was eluted with 2X Laemmli buffer and analyzed for the amount of GTP-bound Rac by immunoblotting using a Rac monoclonal antibody.

Migration assay - Cell migration was assayed using a Transwell cell culture chamber containing polycarbonate membrane inserts with 8 μm pore (Corning Costar Corp.) coated with 0.2% gelatin (24). 48 h after transfection in 6-well plates, the cells were trypsinized, and 5×10^4 cells in 100 μl Dulbecco's modified

Eagle's medium/0.4% fetal bovine serum were added to the upper Transwell chamber. The bottom chamber was filled with 600 μl of media, and the cells were allowed to adhere to the membrane at 37°C for 1 h. VEGF (10 ng/mL), S1P (100 nM) or vehicle was added to the lower chamber, and the assembly was incubated at 37°C for 3 h to allow cell migration. After incubation, the membranes were washed with PBS, and the cells that did not migrate through the membrane were gently removed from the upper surface with a cotton swab. The membranes were then treated with trypsin to detach the migrated cells from the lower surface, and these cells were then counted with a hemocytometer.

Tube formation assay - 250 μl of Matrigel (BD Biosciences, San Jose, CA) was deposited into wells in a 24-well plate and allowed to solidify for 30 min at 37°C . 48 h after siRNA transfection, BAEC were trypsinized, and 3×10^4 cells were added to each Matrigel-coated well. Cells were incubated on Matrigel for 9 hrs at 37°C and imaged by phase contrast microscopy (Nikon Eclipse TS100, 5x objective). Four random fields of view (FOV) per well were examined and photographed by a blinded observer. For quantification purposes, a node was defined as an aggregation of cells from which three or more tube-like structures originated, and a tube referred to a continuous stretch of at least two cells containing no more than two nodes. For each FOV, ImageJ (NIH) was used to measure the total tube length and the length per tube in units of pixels. Each experiment was repeated in nine wells.

Statistical Analysis - All experiments were performed at least three times. Mean values for individual experiments were expressed as mean \pm standard error. Statistical differences were assessed by ANOVA or *t*-test when appropriate. A *p* value of less than 0.05 was considered significant.

RESULTS

VEGF- and S1P-mediated AMPK and ACC phosphorylation - We first studied the effects of VEGF and S1P on the phosphorylation of AMPK and the AMPK

substrate ACC in bovine aortic endothelial cells (BAEC; Fig. 1). After the addition either of VEGF (10 ng/ml) or S1P (100 nM) to BAEC, AMPK phosphorylation increases within 1 min of agonist addition, reaching a maximum ~2.5-fold increase by 5 min, with a gradual return to basal levels at ~30 min following VEGF or S1P addition (Fig. 1A and 1B). Immunoblots probed with a phospho-specific ACC antibody revealed a similar time course for ACC phosphorylation, reaching a peak ~3-fold increase in response to both agonists that gradually returned to baseline after ~30 min following VEGF or S1P addition. We next analyzed the dose response to VEGF and S1P for both AMPK and ACC phosphorylation. Fig. 1C shows immunoblots of BAEC lysates from cells treated for 5 min with increasing concentrations of VEGF or S1P, and probed with antibodies directed against phospho-AMPK and phospho-ACC; total AMPK and ACC levels serve as the control in this immunoblot analysis. The dose response for VEGF-induced AMPK and ACC phosphorylation demonstrated an EC_{50} of ~1 ng/ml; S1P-induced phosphorylation of both targets showed an EC_{50} of ~20 nM; these values fall within the physiological range seen for many other endothelial responses for VEGF and S1P (20). Together, these data indicate that both VEGF and S1P induce the reversible receptor-mediated phosphorylation of AMPK and its substrate ACC in endothelial cells.

siRNA-mediated down-regulation of VEGFR2 and inhibition of tyrosine kinases and PI-3-Kinase in VEGF- and S1P-mediated AMPK and ACC phosphorylation - Previous work from our laboratory (30) and others (31) have observed cross-talk between VEGF and S1P receptors in mediating intracellular endothelial responses. Indeed, it has been previously reported that S1P responses are mediated by VEGF receptor transactivation (31). We explored the possibility of S1P-mediated transactivation of the VEGF receptor 2 (VEGFR2) in promoting AMPK and ACC phosphorylation by using siRNA directed against VEGFR2. BAEC were transfected with duplex siRNAs specific for VEGFR2 (32), and the effects on siRNA-mediated

VEGFR2 knockdown on VEGF- and S1P-induced AMPK and ACC phosphorylation were analyzed (Fig. 2A). VEGFR2 siRNA effectively abrogated AMPK and ACC phosphorylation in response to VEGF, but this siRNA did not affect phosphorylation in response to S1P. These findings indicate that VEGF, but not S1P, acts through the VEGFR2 to activate AMPK and ACC phosphorylation, and argue against S1P-mediated VEGFR2 transactivation as an essential component of S1P-mediated AMPK activation.

We next used a series of pharmacological inhibitors to assess the role of tyrosine kinases and PI-3-kinase (PI3K) in VEGF- and S1P-mediated activation of AMPK and ACC. BAEC were stimulated with agonists following pretreatment either with the broad spectrum tyrosine kinase inhibitor genistein; with the Src tyrosine kinase inhibitor PP2; with the PI3K inhibitor wortmannin; with the calcineurin inhibitor cyclosporine; or with the vehicle as a control (Fig. 2B-D). We found that genistein and PP2 blocked VEGF-induced AMPK and ACC phosphorylation, but did not affect S1P-induced AMPK and ACC phosphorylation. In contrast, pretreatment of BAEC with the PI3K inhibitor wortmannin did not affect AMPK or ACC phosphorylation in response to VEGF (data not shown), but wortmannin pretreatment significantly *increased* phosphorylation of both proteins in response to S1P ($42.4 \pm 18\%$ increase compared with vehicle-pretreated, $n = 3$, $p < 0.05$) (Fig. 2C and 2D). We found that the p38 inhibitor SB203580 had no effect in either VEGF- or S1P-induced AMPK or ACC phosphorylation, with positive controls affirming that p38 phosphorylation was partially blocked under these conditions (Fig. 2C) (33).

Effects of CaMKK inhibition on VEGF- and S1P-mediated AMPK phosphorylation pathways - Both VEGF and S1P increase intracellular calcium in endothelial cells (20), and we sought to characterize a possible calcium-dependent upstream kinase responsible for both VEGF- and S1P-induced AMPK phosphorylation. BAEC incubated with the specific CaMKK inhibitor STO-609 (34, 35) did not

demonstrate agonist-stimulated AMPK and ACC phosphorylation in response to either VEGF or S1P (Fig. 3A). We next designed and validated siRNA targeting bovine the β isoform of CaMKK; transfection with this siRNA severely impaired both VEGF- and S1P-induced AMPK and ACC phosphorylation (Fig. 3B). These findings suggest that CaMKK may link VEGF- and S1P-activated pathways upstream of AMPK phosphorylation

siRNA-mediated down-regulation of AMPK impairs agonist-mediated eNOS and Akt activation - We next used siRNA approaches to explore the role of AMPK in VEGF- and S1P-mediated eNOS and Akt activation in BAEC. Pretreatment of endothelial cells with the potent and selective AMPK inhibitor Compound C (36) inhibited ACC phosphorylation in response to both agonists, and also attenuated VEGF- and S1P-induced eNOS phosphorylation at its activating serine 1179 site without affecting ERK1/2 phosphorylation (Fig. 4A). We then designed and validated a duplex siRNA construct targeting the catalytic α -subunit of AMPK; immunoblotting for total AMPK and for phospho-ACC confirmed $\sim 90\%$ down-regulation of AMPK expression (Fig. 4C). As shown in Figure 4B, down-regulation of AMPK attenuated both VEGF- and S1P-mediated enhancement in eNOS activity, as determined by the intracellular formation of L-[^3H]citrulline from L-[^3H]arginine ($49 \pm 14\%$ decrease in VEGF-induced eNOS activity for AMPK siRNA compared with control siRNA; $43 \pm 19\%$ decrease for S1P-induced eNOS activity; $n = 4$ independent experiments performed in duplicate, $p < 0.05$ for both). siRNA-mediated AMPK knockdown significantly attenuated both VEGF- and S1P-induced eNOS ser1179 phosphorylation compared with control siRNA-treated cells (Fig. 4C and 4D).

Relative roles of AMPK and Akt in agonist-mediated eNOS activation - After identifying AMPK as a critical component of the pathway involved in VEGF- and S1P-induced eNOS activity, we analyzed the relationship between AMPK and another important eNOS kinase, Akt, to determine

how these two kinases may interact in regulating eNOS. As shown in Fig. 5, AMPK siRNA significantly impaired the VEGF- and S1P-mediated phosphorylation of Akt at its serine 473 site, and also blocked phosphorylation of the kinase Akt substrate glycogen synthase kinase-3- β (GSK3- β), suggesting that AMPK lies upstream of Akt in this pathway. We next designed and validated duplex siRNA targeting constructs specific for Akt1, the predominant Akt isoform in endothelial cells (37, 38); immunoblotting for total Akt1 confirmed $\sim 80\text{-}90\%$ knockdown of Akt1, and GSK3- β phosphorylation was efficiently blocked following siRNA-mediated Akt1 knockdown (Fig. 6B and 6C). BAEC transfected with Akt1 siRNA showed a significant decrease in eNOS activity; as shown in Fig. 6A, there was a $48 \pm 5\%$ decrease in eNOS activity in Akt1 siRNA-versus control siRNA-transfected cells in response to VEGF, and a $37 \pm 11\%$ decrease in eNOS activity in response to S1P ($n = 3$, $p < 0.05$ for both). There was also an accompanying decrease in eNOS ser1179 phosphorylation in Akt1 siRNA-transfected cells (Fig. 6B and 6C; for VEGF, there was a $40 \pm 13\%$ reduction in eNOS ser1179 phosphorylation in Akt1 siRNA- versus control siRNA-transfected cells; for S1P, there was a $39 \pm 23\%$ decrease in agonist-mediated eNOS ser1179 phosphorylation; $n = 4$, $p < 0.05$ for both). Importantly, siRNA-mediated Akt1 knockdown did *not* affect either VEGF- or S1P-induced AMPK phosphorylation (Fig. 6B and 6C). These findings suggest that AMPK lies upstream of Akt in VEGF- and S1P-mediated eNOS activation, and indicate that Akt might act as an effector of AMPK in this response.

Role of Rac1 in agonist-modulated, AMPK-mediated eNOS activation - The small GTPase Rac1, which functions as a molecular switch by cycling between an inactive GDP-bound form and an active GTP-bound form, is a well-characterized regulator of the actin cytoskeleton, but whose roles in the Akt/PI3K pathway remain controversial (27, 39, 40). We have previously shown that Rac1 is a key determinant of Akt phosphorylation in response to S1P (27). In the present studies,

we explored the role of Rac1 in modulation of AMPK responses involved in eNOS activation (Fig. 7). BAEC were transfected with either control or AMPK siRNA, and agonist-induced activation of Rac1 was measured in the cell lysates by pull-down of activated GTP-Rac1. We observed that siRNA-mediated AMPK knockdown impaired Rac1 activity in response to both S1P ($53 \pm 17\%$ decrease versus control siRNA; $n = 3$, $p < 0.02$) and VEGF ($48 \pm 21\%$ decrease; $n = 3$, $p < 0.05$), indicating that siRNA-mediated AMPK knockdown attenuates agonist-induced Rac1 activation. We next transfected BAEC with Rac1 siRNA (27), and found that siRNA-mediated Rac1 knockdown significantly impaired both VEGF- and S1P-stimulated phosphorylation of the AMPK substrate ACC and of eNOS, but *without* affecting phosphorylation of AMPK (Fig. 8).

Caveolin-1 regulates AMPK phosphorylation - After identifying a role for Rac1 as a signaling molecule downstream of AMPK, we next explored the relationship between AMPK and the scaffolding/regulatory protein caveolin-1. We previously reported that siRNA-mediated caveolin-1 knockdown significantly enhances both Rac1 activity and Akt phosphorylation (24). To explore the possible role for caveolin-1 in AMPK responses, we transfected BAEC with caveolin-1 siRNA (24) and analyzed the cell lysates in immunoblots probed with phospho-AMPK and phospho-GSK3- β specific antibodies (Fig. 9). As we found previously, caveolin-1 knockdown significantly increased GSK3- β phosphorylation. Importantly, siRNA-mediated caveolin-1 knockdown also reproducibly potentiated basal AMPK phosphorylation (2.5 ± 0.2 -fold increase in basal phosphorylation compared to control siRNA-treated cells, $p < 0.01$), and also enhanced the agonist-mediated response to VEGF ($40 \pm 10\%$ increase in AMPK phosphorylation, $p < 0.01$), as well as S1P ($44 \pm 11\%$ increase, $p < 0.01$) as shown in Figs. 9B and 9C. This finding suggests that caveolin-1 acts as a negative regulator of agonist-mediated AMPK phosphorylation in endothelial cells.

Role of AMPK pathway in VEGF- and S1P-mediated endothelial cell migration - We have previously shown that Rac1 activity is critical for endothelial migration in response to S1P (24, 27) and we hypothesized that AMPK modulates both VEGF- and S1P-induced endothelial cell migration through the Rac1-Akt-eNOS pathway described above. Fig. 10 shows the results of a cell migration assay using a Transwell cell culture chamber containing BAEC transfected with control siRNA or with siRNA constructs targeting caveolin-1, AMPK, Akt1, or eNOS, as shown. Transfection of BAEC with these siRNA targeting constructs led to significant and specific knockdown of their cognate proteins (Fig. 10A). As shown in Figure 10B, agonist-enhanced endothelial cell migration was significantly reduced in cells transfected with the AMPK siRNA ($43 \pm 10\%$ decrease in VEGF-stimulated cell migration relative to control siRNA-transfected cells; $46 \pm 14\%$ decrease for S1P-induced migration relative to control siRNA-transfected cells; $n = 3$, $p < 0.05$). Agonist-induced cell migration was also attenuated by Rac1 siRNA ($42 \pm 8\%$ attenuation of the response to VEGF, and $39 \pm 7\%$ inhibition for S1P; $n = 3$, $p < 0.05$ for both). There was a similar attenuation of the migration response to VEGF ($31 \pm 13\%$ decrease) and S1P ($36 \pm 17\%$) following transfection of Akt1 siRNA ($n = 3$, $p < 0.05$ for both agonists). Finally, eNOS siRNA transfection led to a marked reduction in migration responses to VEGF ($44 \pm 11\%$) as well as to S1P ($48 \pm 14\%$) ($n = 3$, $p < 0.004$ for both VEGF and S1P responses following eNOS siRNA transfection compared to control siRNA transfection, analyzed by ANOVA).

AMPK mediates endothelial tube formation via Rac1 and eNOS signaling - After identifying a role for AMPK and several of its signaling partners in endothelial cell migration, we next explored the consequences of knockdown of AMPK and AMPK target proteins in the endothelial cell tube formation assay, an extensively-validated *in vitro* model for angiogenesis (41, 42). siRNA-transfected BAEC were plated on Matrigel (41, 42) and allowed to form capillary-like tubes for 9 h; the tubes were then photographed and

analyzed using novel quantification parameters. Compared to cells transfected with control siRNA, BAEC transfected with siRNA constructs targeting AMPK, Rac1, or eNOS siRNA – but not caveolin-1 – exhibited a significantly reduction in tube formation. As shown in Fig. 11B, there was a $59 \pm 6\%$ reduction in average total tube length per field of view in cells transfected with AMPK siRNA, a $37 \pm 7\%$ reduction in cells transfected with Rac1 siRNA, and a $46 \pm 4\%$ reduction in cells transfected with eNOS siRNA, compared with cells transfected with control siRNA ($n = 9$ wells each, $p < 0.02$ for all conditions). We also measured the length of individual tubes, and then performed population analyses for each experimental condition. In analyzing this quantification parameter, we found that cells that had been transfected with AMPK, Rac1, or eNOS siRNA had shorter individual tubes, (Fig. 11C), as well as a reduction in the aggregate length of endothelial tubes.

DISCUSSION

We have pursued pharmacological approaches along with siRNA-mediated knockdown methods to study the molecular mechanisms involved in VEGF and S1P signaling to AMPK. In these studies, we have explored the upstream modulators of agonist-mediated AMPK phosphorylation and have identified a novel AMPK→Rac1→Akt pathway that functions as a critical determinant of eNOS activity, as well as endothelial migration and tube formation, in the vascular endothelium.

Although traditionally thought to be regulated by the cellular energy state alone, AMPK is now known to be activated by calcium-dependent signaling pathways (for a review, see Ref. 43). In endothelial cells, AMPK is known to phosphorylate the ser1179 site on eNOS, thereby increasing the V_{\max} of the enzyme and its sensitivity to calcium and calmodulin (8). Both the polypeptide growth factor VEGF and the lipid mediator S1P are known to activate eNOS in endothelial cells in part through mobilization of calcium (20), but previous studies have not clearly demonstrated

AMPK-dependent pathways in these agonist-mediated responses. Although a recent report has implicated AMPK in VEGF-stimulated endothelial NO production (18), the mechanisms linking VEGF stimulation with AMPK and eNOS activation were not explored. Furthermore, it has not been shown whether S1P can also regulate AMPK upstream of eNOS activation. In the present studies we conclusively identify AMPK as a mediator of VEGF- and S1P-mediated eNOS activation, in the absence of any other known AMPK regulators. In BAEC, VEGF and S1P were found to reversibly phosphorylate AMPK at its activation site, thr172, along with phosphorylation of the AMPK substrate ACC (Fig. 1). We found that this phosphorylation occurred at EC_{50} values (~ 1 ng/ml for VEGF and ~ 10 - 20 nM for S1P) characteristic of those observed with other receptor-mediated effects of these agonists (reviewed in Ref. 20). In contrast to our findings, Zou *et al.* found that VEGF did not affect AMPK activity either administered alone or in combination with the AMPK activator peroxynitrite (44), and Nagata *et al.* did not observe a significant role for AMPK in VEGF-mediated angiogenesis under normoxic conditions (12). We note that in these studies, cells were stimulated with VEGF at concentrations of 50 ng/mL (44, 12) for as long as 6 hours (12), a dose and time point at which we also did not observe the stimulatory effects of VEGF upon AMPK.

In contrast to the VEGF receptor tyrosine kinase, S1P is known to facilitate its endothelial cell functions by interacting with G protein-coupled S1P receptors (45, 46). Despite these differential modes of receptor activation, we have previously found that the Src tyrosine kinase inhibitor PP2 blocks S1P-mediated Rac1 activation and Akt phosphorylation (27), thereby implicating tyrosine kinases in S1P-mediated signal transduction. In the present studies, however, we observed that PP2, as well as the broad-spectrum tyrosine kinase inhibitor genistein, diminished VEGF-mediated AMPK and ACC phosphorylation, but did not affect these responses mediated by S1P (Fig. 2B). Taken together with our previous work, it appears

that the role of Src in endothelial cells is agonist-dependent, as Src appears to lie upstream of AMPK when cells are stimulated by VEGF, but downstream of AMPK when cells are stimulated by S1P. We found further that VEGFR2 siRNA impaired VEGF- but not S1P-mediated AMPK and ACC phosphorylation (Fig. 2A), thereby indicating that VEGFR2 does not play a role in the S1P-stimulated AMPK pathway. In addition to the VEGFR2 and tyrosine kinases, our work identifies PI3K as another important locus of differential regulation of AMPK by VEGF versus S1P: whereas the PI3K inhibitor wortmannin did not affect VEGF-induced AMPK and ACC phosphorylation at doses sufficient for inhibition of Akt activation, wortmannin substantially increased phosphorylation of both targets in response to S1P (Fig. 2C). These results suggest divergent receptor-modulated PI3K-independent pathways upstream of AMPK (47), and lead us to speculate that although both agonists activate AMPK in a PI3K-independent manner, S1P – but not VEGF – might also activate a competitive PI3K-dependent pathway whose inhibition results in hyperphosphorylation of AMPK. Although VEGF and S1P activate differential pathways upstream of AMPK, our studies implicate CaMKK β as a common upstream modulator of AMPK phosphorylation. Indeed, both the CaMKK inhibitor STO-609 and CaMKK β siRNA effectively abrogated both VEGF- and S1P-mediated AMPK and ACC phosphorylation (Fig. 3). However, the complexities of calcium/calmodulin-dependent responses in AMPK signaling, and the fact that eNOS itself is modulated by calcium/calmodulin, together hamper our ability to discern the detailed mechanisms whereby CaMKK β regulates receptor-dependent signaling to eNOS.

The question of whether AMPK is a critical component of the receptor-modulated signaling pathways leading to eNOS activation appears to vary depending on the particular agonist. For example, both AICAR-induced (17) and receptor-mediated activation of eNOS by histamine (47), adiponectin (12), or estradiol (48) depend at least partially upon

AMPK. By contrast, AMPK is not involved in other receptor-mediated cell signaling pathways that result in eNOS activation or nitric oxide release, such as those stimulated by insulin (11), thrombin (36), or bradykinin (49). In these studies, we observed that either pharmacologic inhibition or siRNA-mediated down-regulation of the catalytic subunit of AMPK impaired both eNOS activity and eNOS phosphorylation at its activating ser1179 site in response to either VEGF or S1P (Fig. 4). These results establish that AMPK is a critical component of the eNOS-activating pathways modulated by both VEGF and S1P.

The critical role of AMPK in VEGF- and S1P-induced eNOS activity and phosphorylation led us to explore the role of another eNOS kinase, Akt. There is a complex and incompletely understood relationship between AMPK and Akt in both cardiac myocytes and endothelial cells, with several recent reports highlighting the importance of AMPK-Akt cross-talk in modulating agonist-mediated AMPK activities (16, 17, 50, 51). Horman et al. recently proposed a mechanism in rat hearts whereby insulin treatment decreased AMPK thr172 phosphorylation in an Akt-dependent manner, thereby identifying Akt as a negative regulator of AMPK activity in response to insulin (50). Similarly, Soltys *et al.* found that activation of Akt1 prevents activation of AMPK by LKB1 in isolated cardiac myocytes by phosphorylating the regulatory ser485/491 site on AMPK (51). By contrast, our studies in BAEC with Akt1 siRNA (Fig. 6) argue strongly against an upstream role for Akt in VEGF- and S1P-mediated AMPK activation, as Akt1 knockdown impaired eNOS activity and ser1179 phosphorylation *but did not affect AMPK phosphorylation in response to either agonist*. It may be that the Akt-AMPK interaction depends importantly upon the cell type and the specific receptor-mediated pathway at play. Whether Akt lies downstream and not just parallel to AMPK is also controversial and appears to be cell type-specific and agonist-dependent. For example, Morrow *et al.* found that expression of dominant negative AMPK had no effect on

AICAR- stimulated Akt phosphorylation in human aortic endothelial cells (17). By contrast, Ouchi *et al.* showed that inhibition of AMPK signaling with dominant negative constructs suppressed adiponectin-induced Akt phosphorylation, suggesting that Akt lies downstream of AMPK in adiponectin-activated endothelial cell pathways (16). Our data using AMPK siRNA are consistent with these latter observations, in which our studies clearly establish that AMPK functions upstream of Akt in VEGF- and S1P-mediated eNOS activation (Fig. 5), and thereby implicate an AMPK→Akt→eNOS pathway in response to these agonists. It is worth noting that siRNA-mediated knockdown of Akt1 did not lead to AMPK or ACC hyperphosphorylation, in contrast to the hyperphosphorylation effect seen with the PI3K inhibitor wortmannin. We speculate that this difference between the effects of wortmannin versus Akt1 siRNA may reflect Akt-independent signaling downstream of PI3K, perhaps involving the MAPK pathway, as has been proposed in a number of recent reports (52, 53). Further studies will be necessary to determine whether AMPK can directly activate eNOS in a pathway that does not involve Akt.

The present studies have also implicated Rac1 in a novel role downstream of the activation of AMPK. Rac1 has been previously implicated in a broad range of both VEGF- and S1P- mediated cellular responses in vascular endothelial cells, including nitric oxide release, migration, and angiogenesis (54). We have recently reported that S1P-enhanced Rac1 activation is required for the activation of Akt and eNOS (27). Our identification of an AMPK-Akt-eNOS axis in VEGF- and S1P-treated endothelial cells therefore led us to hypothesize that Rac1 might play a role in the AMPK-mediated modulation of Akt and eNOS. We discovered that siRNA-mediated AMPK knockdown significantly impaired both VEGF- and S1P-induced Rac1 activation (Fig. 7), suggesting that AMPK is required for receptor-mediated Rac1 activation. By contrast, siRNA-mediated Rac1 knockdown impaired VEGF- and S1P-induced eNOS and ACC

phosphorylation, but had no effect on agonist-induced AMPK phosphorylation (Fig. 8), thereby identifying Rac1 as a critical regulator of downstream AMPK targets, but not of AMPK itself. Taken together with our recent finding that Rac1 knockdown also attenuates phosphorylation of Akt and its substrate GSK3-β (27), the present studies suggest that Rac1 might act as an AMPK effector in modulating AMPK-dependent regulation of both ACC and the agonist-mediated Akt/eNOS pathway in endothelial cells. To our knowledge, this is the first report of a link between AMPK and Rac1. Indeed, it is tempting to speculate that AMPK-mediated regulation of Rac1 might play a role in cellular defense against oxidative stress, as both proteins have been implicated in endothelial cell redox signaling and cardioprotection (55, 56).

In addition to AMPK, caveolin-1 represents another important regulator of Rac1 activity. We have previously reported that siRNA-mediated knockdown of caveolin-1 significantly enhances both Rac1 activity and Akt phosphorylation, suggesting a mechanism whereby caveolin-1 negatively regulates Rac1, which in turn modulates the PI3K/Akt/eNOS pathway in endothelial cells (24). In the present studies, we were intrigued to find that siRNA-mediated caveolin-1 knockdown enhanced AMPK phosphorylation both in the basal state and in response to VEGF and S1P (Fig. 9), thereby suggesting that caveolin-1 also negatively regulates AMPK activity. Interestingly, the increase in AMPK phosphorylation seen with caveolin-1 knockdown appeared to effectively “uncouple” VEGF- and S1P-stimulated AMPK phosphorylation, suggesting that abrogation of the inhibitory effect of caveolin-1 on AMPK phosphorylation with caveolin-1 siRNA might eclipse the otherwise stimulatory effect of these receptor-dependent AMPK agonists. We note that other kinases such as protein kinase A (57) as well as phosphoprotein phosphatases (58) have been implicated in ACC regulation. It is plausible that these other mechanisms may play a role in enhancing ACC activity when AMPK phosphorylation is stimulated following

caveolin-1 knockdown. Importantly, we also did not observe statistically significant differences in eNOS phosphorylation or activity in caveolin-1 siRNA- versus control siRNA-transfected cells (data not shown), consistent with our previous work (24). We note that although eNOS is a target of AMPK, eNOS activation depends upon many other signaling proteins including protein kinase A (59) and the protein phosphatase PP2A (60), whose role in eNOS regulation may counterbalance the anticipated increase in eNOS phosphorylation after caveolin-1 knockdown. Caveolin-1 may even directly interact with these other eNOS regulators in a way that would attenuate an increase in eNOS phosphorylation. For example, Li *et al.* (61) have reported that overexpression of caveolin-1 inhibits protein phosphatases PP1 and PP2A in prostate cancer cells. Possibly, siRNA-mediated caveolin-1 knockdown might remove this inhibitory effect on these phosphatases, and thereby enhance the dephosphorylation of eNOS, thus attenuating the enhancement in eNOS phosphorylation consequent to activation of AMPK following caveolin-1 knockdown. Both the complex upstream regulation of eNOS and the pleiotropic effects of caveolin-1 in endothelial cells may explain why caveolin-1 knockdown does not significantly affect eNOS phosphorylation at ser1179 despite a robust enhancement of AMPK phosphorylation. Further studies of agonist-modulated AMPK pathways may help to further define the inhibitory interaction between caveolin-1 and AMPK.

Our studies also contribute insights into the molecular mechanisms involved in eNOS-dependent endothelial migration and tube formation, two key endothelial functional responses involved in many processes including wound healing, vascular development, and angiogenesis (41, 62). Both VEGF (63) and S1P (64) are known to stimulate endothelial cell migration, mediated in part through eNOS signaling; our study provides new information implicating AMPK in the modulation of eNOS activation associated with agonist-induced cell migration

responses (Fig. 10). Extending our previous work that implicated Rac1 in endothelial migration (24), these studies have also identified a context for Rac1 as an AMPK mediator in regulating endothelial migration. We have also exploited siRNA-based approaches to explore the roles of AMPK and its modulators in endothelial tube formation upon the basement membrane-like matrix Matrigel. The Matrigel tube formation assay is an extensively-validated method that permits the quantitative analysis of the propensity for cultured endothelial cells to form capillary-like structures, providing a useful model for angiogenesis (41, 65). Using rigorous quantification methods, we found that BAEC transfected with AMPK, Rac1, or eNOS siRNA formed less extensive tubular networks as well as shorter individual tubes (Fig. 11), thereby indicating that eNOS is required for adequate endothelial tube formation in an AMPK- and Rac1-dependent manner.

With the advent of studies implicating alternative, AMP-independent pathways of AMPK activation (43), it now appears that the AMPK system functions to respond not only to cell autonomous signs of stress such as AMP, but also to circulating factors that act as regulators of cellular function in both physiologic and pathophysiologic states. As key determinants of many cellular processes in endothelial cells, VEGF and S1P represent intriguing new stimuli for AMPK activation. These studies have demonstrated that the potent eNOS agonists VEGF and S1P differentially phosphorylate and thereby activate AMPK in vascular endothelial cells, and establish a central role for AMPK in VEGF- and S1P-mediated eNOS activity. We identify for the first time an AMPK→Rac1→Akt pathway that functions as a critical determinant of eNOS activity and endothelial migration and tube formation in endothelial cells. These studies have provided new insights into the molecular mechanisms linking extracellular signals with AMPK in the modulation of eNOS activation in the vascular endothelium.

REFERENCES

1. Hardie, D. J., and Carling, D. (1997) *Eur. J. Biochem.* **246**, 259-273
2. Hurley, R. L., Anderson, K. A., Franzoni, J. M., Kemp, B. E., Means, A. R., and Witters, L. A. (2005) *J. Biol. Chem.* **280**, 29060--29066
3. Hawley, S. A., Pan, D. A., Mustard, K. J., Ross, L., Bain, J., Edelman, A. M., Frenguelli, B. G., and Hardie, D. G. (2005) *Cell Met.* **2**, 9-19
4. Shaw, R. J., Kosmatka, M., Bardeesy, N., Hurley, R. L., Witters, L. A. DePinho, R. A., and Cantley, L. C. (2004) *Proc. Natl. Acad. Sci. U. S. A.* **101**, 3329-3335
5. Sambandam, N., and Lopaschuk, G. D. (2003) *Progress in Lipid Research* **42**, 238-256
6. Reznick, R. M., and Shulman, G. I. (2006) *J. Physiol.* **574**, 33-39
7. Carling, D., Clarke, P. R., Zammit, V. A., and Hardie, D. G. (1989) *Eur. J. Biochem.* **186**, 129-136
8. Chen, Z. P., Mitchelhill, K. I., Michell, B. J., Stapleton, D., Rodriguez-Crespo, I., Witters, L. A., Power, D. A., Ortiz de Montellano, P. R., and Kemp, B. E. (1999) *FEBS Lett.* **443**, 285-289
9. Zou, M. H., Kirkpatrick, S. S., Davis, B. J., Nelson, J. S., Wiles, W. G 4th, Schlattner, U., Neumann, D., Brownlee, M., Freeman, M. B., and Goldman, M. H. (2004) *J. Biol. Chem.* **279**, 43940-43951
10. Yamauchi, T., Kamon, J., Minokoshi, Y., Ito, Y., Waki, H., Uchida, S., Yamashita, S., Noda, M., Kita, S., Ueki, K., Eto, K., Akanuma, Y., Froguel, P., Foufelle, F., Ferre, P., Carling, D., Kimura, S., Nagai, R., Kahn, B. B., and Kadowaki, T. (2002) *Nat. Med.* **8**, 1288-1295
11. Chen, H., Montagnani, M., Funahashi, T., Shimomura, I., and Quon, M. J. (2003) *J. Biol. Chem.* **278**, 45021-45026
12. Nagata, D., Mogi, M., and Walsh, K. (2003) *J. Biol. Chem.* **278**, 31000-31006
13. Sun, W., Lee, T. S., Zhu, M., Gu, C., Wang, Y., Zhu, Y., and Shyy, J. Y. (2006) *Circulation* **114**, 2655-2662
14. Quintero, M., Colombo, S. L., Godfrey, A., and Moncada, S. (2006) *Proc. Natl. Acad. Sci. U. S. A.* **103**, 5379-84
15. Fulton, D., Gratton, J.-P., McCabe, T. J., Fontana, J., Fujio, Y., Walsh, K., Franke, T. F., Papapetropoulos, A., and Sessa, W. C. (1999) *Nature* **399**, 597-601
16. Ouchi, N., Kobayashi, H., Kihara, S., Kumada, M., Sato, K., Inoue, T., Funahashi, T., and Walsh, K. (2004) *J. Biol. Chem.* **279**, 1304-1309
17. Morrow, V. A., Foufelle, F., Connell, J. M., Petrie, J. R., Gould, G. W., and Salt, I. P. (2003) *J. Biol. Chem.* **278**, 31629-31639
18. Reihill, J. A., Ewart, M., Hardie, D. G., and Salt, I. P. (2007) *Biochem. Biophys. Res. Commun.* **354**, 1084-1088
19. Igarashi, J., Bernier, S. G., and Michel, T. (2001) *J. Biol. Chem.* **276**, 12420-12426
20. Dudzinski, D. M., Igarashi, J., Greif, D., and Michel, T. (2006) *Annu. Rev. Pharmacol. Toxicol.* **46**, 235-276
21. Yamada, E. (1955) *J. Biophys. Biochem. Cytol.* **1**, 445-458
22. Rothberg, K. G., Heuser, J. E., Donzell, W. C., Ying, Y. S., Glenney, J. R., and Anderson, R. G. (1992) *Cell* **68**, 673-682
23. Parton, R. G. (1996) *Curr. Opin. Cell Biol.* **8**, 542-548
24. Gonzalez, E., Nagiel, A., Lin, A. J., Golan, D. E., and Michel, T. (2004) *J. Biol. Chem.* **279**, 40659-40669
25. Kinsella, B. T., Erdman, R. A., and Maltese, W. A. (1991) *J. Biol. Chem.* **266**, 9786-9794
26. Burrige, K., and Wennerberg, K. (2004) *Cell* **116**, 167-179
27. Gonzalez, E., Kou, R., and Michel, T. (2006) *J. Biol. Chem.* **281**, 3210-3216
28. Elbashir, S. M., Harborth, J., Lendeckel, W., Yalcin, A., Weber, K., and Tuschl, T. (2001) *Nature* **411**, 494-498
29. Balligand, J. L., Kobzik, L., Han, X., Kaye, D. M., Belhassen, L., O'Hara, D. S., Kelly, R. A., Smith, T. W., and Michel, T. (1995) *J. Biol. Chem.* **270**, 14582-14586
30. Igarashi, J., Erwin, P. A., Dantas, A. P., Chen, H., and Michel, T. (2003) *Proc. Natl. Acad. Sci. U. S. A.* **100**, 10664-10669

31. Tanimoto, T., Jin, Z. G., and Berk, B. C. (2002) *J. Biol. Chem.* **277**, 42997–43001
32. Kou, R., SenBanerjee, S., Jain, M. K., and Michel, T. (2005) *Biochemistry* **44**, 15064–15073
33. Kang, Y. J., Seit-Nebi, A., Davis, R. J., Han, J. (2006) *J. Biol. Chem.* **281**, 26225–26234
34. Tokumitsu, H., Inuzuka, H., Ishikawa, Y., Ikeda, M., Saji, I., and Kobayashi, R. (2002) *J. Biol. Chem.* **277**, 15813–15818
35. Tokumitsu, H., Inuzuka, H., Ishikawa, Y., and Kobayashi, R. (2003) *J. Biol. Chem.* **278**, 10908–10913
36. Zhou, G., Myers, R., Li, Y., Chen, Y., Shen, X., Fenyk-Melody, J., Wu, M., Ventre, J., Doebber, T., Fujii, N., Musi, N., Hirshman, M. F., Goodyear, L. J., and Moller, D. E. (2001) *J. Clin. Invest.* **108**, 1167–1174
37. Chen, J., Somanath, P. R., Razorenova, O., Chen, W. S., Hay, N., Bornstein, P., and Byzova, T. V. (2005) *Nat. Med.* **11**, 1188–1196
38. Somanath, P. R., Razorenova, O. V., Chen, J., Byzova, T. V. (2006) *Cell Cycle* **5**, 512–508
39. Lee, M. J., Thangada, S., Paik, J. H., Sapkota, G. P., Ancellin, N., Chae, S. S., Wu, M., Morales-Ruiz, M., Sessa, W. C., Alessi, D. R., and Hla, T. (2001) *Mol. Cell* **8**, 693–704
40. Toliyas, K. F., Cantley, L. C., and Carpenter, C. L. (1995) *J. Biol. Chem.* **270**, 17656–17659
41. Auerbach, R., Lewis, R., Shinnars, B., Kubai, L. & Akhtar, N. (2003) *Clin. Chem.* **49**, 32–40
42. Grant, D. S., Kibbey, M. C., Kinsella, J. L., Cid, M. C. & Kleinman, H. K. (1994) *Pathol. Res. Pract.* **190**, 854–63
43. Birnbaum, M. J. (2005) *Mol. Cell* **19**, 289–296
44. Zou, M. H., Hou, X. Y., Shi, C. M., Kirkpatrick, S., Liu, F., Goldman, M. H., and Cohen, R. A. (2003) *J. Biol. Chem.* **278**, 34003–34010
45. Wang, F., van Brocklyn, J. R., Hobson, J. P., Movafagh, S., Zukowska-Grojec, Z. (1999) *J. Biol. Chem.* **275**, 35343–35350
46. Petrova, T. V., Makinen, T., and Alitalo, K. (1999) *Exp. Cell Res.* **253**, 117–130
47. Hors, B., Halldorsson, H., and Thorgeirsson, G. (2004) *FEBS Lett.* **573**, 175–180
48. Schulz, E., Anter, E., Zou, M. H., and Keaney, Jr., J. F. (2005) *Circulation* **111**, 3473–3480
49. Mount, P. F., Hill, R. E., Fraser, S. A., Levidiotis, V., Katsis, F., Kemp, B. E., and Power, D. A. (2005) *Am. J. Physiol. Renal Physiol.* **289**, F1103–F1115
50. Horman, S., Vertommen, D., Heath, R., Neumann, D., Mouton, V., Woods, A., Schlattner, U., Wallimann, T., Carling, D., Hue, L., and Rider, M. H. (2006) *J. Biol. Chem.* **281**, 5335–5340
51. Soltys, C., Kovacic, S., Dyck, J. (2006) *Am. J. Physiol. Heart Circ. Physiol.* **290**, H2472–H2479
52. Qiao, M., Shapiro, P., Kumar, R., and Passaniti, A. (2004) *J. Biol. Chem.* **279**, 42709–18
53. Zhang, Q., Adisheshaiah, P., Kalvakolanu, D. V., Reddy, S. P. (2006) *J. Biol. Chem.* **281**, 10174–10181
54. Seebach, J., Madler, H. J., Wojciak-Stothard, B., Schnittler, H. J. (2005) *Thromb. Haemost.* **94**, 620–629
55. Russell, R. R., Li, J., Coven, D. L., Pypaert, M., Zechner, C., Palmeri, M., Giordano, F. J., Mu, J., Birnbaum, M. J. & Young, L. H. (2004) *J. Clin. Invest* **114**, 495–503.
56. Brandes, R. P. (2003) *Antioxid. Redox Signal.* **5**, 803–11
57. Brownsey, R. W., Boone, A. N., Elliott, J. E., Kulpa, J. E., and Lee, W. M. (2006) *Biochem Soc Trans.* **34(2)**, 223–7
58. Palanivel, R., Veluthakal, R., McDonald, P., and Kowluru, A. (2005) *Endocrine* **26**, 71–7
59. Butt, E., Bernhardt, M., Smolenski, A., Kotsonis, P., Fröhlich, L. G., Sickmann, A., Meyer, H. E., Lohmann, S. M., and Schmidt, H. H. H. W. (2000) *J. Biol. Chem.* **275**, 5179–5187
60. Greif, D. M., Kou, R., Michel, T. (2002) *Biochemistry* **41**, 15845–53
61. Li, L., Ren, C. H., Tahir, S. A., Ren, C., and Thompson, T. C. (2003) *Mol. Cell. Biol.* **23**, 9389–9404
62. BurrIDGE, K., and Wennerberg, K. (2004) *Cell* **116**, 167–179
63. Jozkowicz, A., Dulak, J., Nigisch, A., Funovics, P., Weigel, G., Polterauer, P., Huk, I., Malinski, T. (2004) *Growth Factors* **22**, 19–28
64. Rikitake, Y., Hirata, K., Kawashima, S., Ozaki, M., Takahashi, T., Ogawa, W., Inoue, N., Yokoyama, M. (2002) *Arterioscler. Throm. Vasc. Biol.* **22**, 108–14
65. Folkman, J., Haudenschild, C. (1980) *Nature* **288**, 551–6

FOOTNOTES

*This work was supported by National Institutes of Health Grants HL46457 and GM36259 (to T.M.), and by the Sarnoff Cardiovascular Research Foundation (to Y.C.L.). The authors would like to thank Drs. Eva Gonzalez, Hongjie Chen, Ruqin Kou, Alison Lin, Juliano Sartoretto, and Toru Sugiyama for expert assistance and constructive critique.

The abbreviations used are: AMPK, 5'-AMP-activated protein kinase; ACC, acetyl-CoA carboxylase; BAEC, bovine aortic endothelial cells; DMEM, Dulbecco's modified Eagle's medium; eNOS, endothelial nitric oxide synthase; CaMKK β , calcium/calmodulin-dependent protein kinase kinase β ; siRNA, small interfering RNA; PI, phosphoinositide; PDK, phosphoinositide-dependent kinase; GSK3- β , glycogen synthase kinase-3- β ; VEGF, vascular endothelial growth factor; VEGFR2, VEGF receptor 2; S1P, sphingosine 1-phosphate; AICAR, 5-aminoimidazole-4-carboxamide-1- β -D-ribofuranoside; CsA, cyclosporine A; PAK-1, p21-activated kinase-1; GST, glutathione *S*-transferase; ERK, extracellular signal-regulated kinase; TTL, total tube length; FOV, field of view; a.u., arbitrary units; ANOVA, analysis of variance

FIGURE LEGENDS

Fig. 1. Time course and dose response for VEGF- and S1P- mediated phosphorylation of AMPK and ACC. Panel A shows the results of immunoblots analyzed in BAEC lysates prepared from cells treated with VEGF (10 ng/ml) or S1P (100 nM) for the indicated times. Cell lysates were resolved by SDS-PAGE and probed using antibodies directed against phospho-AMPK, AMPK, phospho-ACC, and ACC, as indicated. The experiment shown is representative of four independent experiments that yielded similar results. Panel B shows the results of densitometric analyses from pooled data, plotting the fold increase of the degree of phosphorylation of AMPK at the times indicated, relative to the signals present in the unstimulated cells. Each data point represents the mean \pm S.E. derived from four independent experiments. Panel C shows the results of immunoblots analyzed in BAEC lysates prepared from cells treated with VEGF or S1P for 5 minutes at the indicated concentrations. Cell lysates were resolved by SDS-PAGE and probed using antibodies directed against phospho-AMPK, AMPK, phospho-ACC, and ACC. The experiment shown is representative of three independent experiments that give equivalent results.

Fig. 2. Differential effects of siRNA-mediated VEGFR2 knockdown and protein kinase inhibitors on VEGF- and S1P-mediated AMPK and ACC phosphorylation. Panel A shows an immunoblot of lysates prepared from BAEC that were transfected either with control (C) or VEGFR2 (V) siRNA, and subsequently treated with VEGF (10 ng/ml) or S1P (100 nM) for the indicated times. Cell lysates were resolved on SDS-PAGE and analyzed in immunoblots probed with phospho-AMPK, AMPK, phospho-ACC, ACC, and VEGFR2-specific antibodies. The immunoblots in panel B show results of experiments exploring the effects of various inhibitors on S1P- and VEGF-mediated phosphorylation responses. BAEC were treated with VEGF, S1P, or their vehicle (\emptyset) for 5 minutes, and immunoblots of cell lysates were probed with the specific antibodies shown. Prior to agonist stimulation, cells were treated for 30 min with the tyrosine kinase inhibitor genistein (100 μ M); the Src inhibitor PP2 (10 μ M); the calcineurin inhibitor cyclosporine A (CsA, 100 nM); the p38 kinase inhibitor SB203580 (1 μ M), or vehicle (-) as noted. In panel C, BAEC were pretreated with wortmannin (1 μ M) or its vehicle, and then treated with S1P for the indicated times. Panel D shows densitometric analysis of pooled data presenting the relative phosphorylation of AMPK after 5-min treatment with VEGF or S1P in the presence or absence of the inhibitors studied in the experiments shown in panels B and C. Each

data point represents the mean \pm S.E. derived from three independent experiments; for the vehicle-, CsA-, and SB203580-pretreated cells, the addition of VEGF and S1P induced a significant increase in AMPK phosphorylation ($p < 0.001$). *, $p < 0.05$ versus vehicle (ANOVA).

Fig. 3. Effects of the CaMKK inhibitor STO-609 or CaMKK siRNA on VEGF- and S1P-induced AMPK and ACC phosphorylation. In Panel A, BAEC lysates were prepared from cells pretreated with STO-609 at the indicated concentrations or its vehicle and then treated with VEGF (10 ng/mL) or S1P (100 nM) for 2 minutes. Cell lysates were resolved by SDS-PAGE and probed using antibodies directed against phospho-AMPK, AMPK, phospho-ACC, and phospho-ERK1/2. Shown are the representative data of three independent experiments. Panel B shows immunoblots of cell lysates prepared from BAEC that had been transfected 48 hrs earlier with control or CaMKK β -specific siRNA. Cell lysates were resolved by SDS-PAGE and probed with the antibodies shown. An anti-CaMKK β antibody was used to confirm siRNA-mediated CaMKK β down-regulation. The experiment was repeated three times with equivalent results.

Fig. 4. Effects of pharmacologic inhibition or siRNA-mediated down-regulation of AMPK upon VEGF- and S1P-mediated eNOS activation. A, BAEC lysates were prepared from cells that had been incubated with Compound C (20 μ M) for 30 min or its vehicle, and then treated with VEGF (10 ng/ml) or S1P (100 nM) for 5 minutes. Cell lysates were resolved by SDS-PAGE and probed using antibodies directed against phospho-ACC, ACC, phospho-eNOS, eNOS, and phospho-ERK1/2. The experiment shown is representative of three independent experiments that gave equivalent results. In panel B, transfected BAEC were assayed for eNOS enzyme activity by incubating the cells with a mixture of unlabeled L-arginine, [3 H]L-arginine, and VEGF (10 ng/ml) or S1P (100 nM) for 1 hr, and cell extracts were processed to quantitate formation of 3 H-citrulline, as detailed in Experimental Procedures. Addition of VEGF and S1P yielded a significant increase in eNOS activity in control siRNA-transfected cells ($p < 0.01$). *, $p < 0.05$ for AMPK α 1 versus control siRNA-transfected cells (ANOVA). C, BAEC transfected with control or AMPK α 1 siRNA were stimulated with VEGF (10 ng/ml) or S1P (100 nM) for the indicated times. Cells were lysed, and phosphorylation of eNOS and ACC were analyzed in the cell lysates in immunoblots probed with antibodies as shown. siRNA-mediated knockdown of AMPK was determined in immunoblots probed with AMPK antibody. D, densitometric analysis of pooled data, quantitating the relative eNOS phosphorylation in control and AMPK α 1 siRNA-transfected cells under basal conditions and after treatment with VEGF or S1P for 5 min. Each data point represents the mean \pm S.E. derived from four independent experiments; the addition of VEGF and S1P induced a significant increase in phosphorylation of eNOS in control siRNA-transfected cells ($p < 0.005$). *, $p < 0.05$ for AMPK α 1 versus control siRNA-transfected cells (ANOVA).

Fig. 5. Effects of siRNA-mediated down-regulation of AMPK on VEGF- and S1P-mediated Akt phosphorylation. In Panel A, BAEC transfected with control or AMPK α 1 siRNA were treated with VEGF (10 ng/m) or S1P (100 nM) for the indicated times. Cell lysates were resolved on SDS-PAGE and analyzed in immunoblots probed with specific antibodies directed against phospho-Akt, Akt, phospho-GSK3- β , GSK3- β , and AMPK. Shown are the results of a representative experiment that was repeated four times with equivalent results. B, pooled data plotting the ratio between the signal intensity of phospho-Akt and total Akt or phospho-GSK3- β and total GSK3- β as determined by densitometry. Each point in the graph represents the mean \pm S.E. of four independent experiments. *, $p < 0.05$ versus control siRNA-transfected cells (using ANOVA).

Fig. 6. Effects of siRNA-mediated down-regulation of Akt1 on VEGF- and S1P-mediated eNOS activation and AMPK phosphorylation. *A*, BAEC transfected with control or Akt1 siRNA were assayed for eNOS enzyme activity as described above. The addition of VEGF and S1P induced a significant increase in eNOS activity in control siRNA-transfected cells ($p < 0.01$). *, $p < 0.05$ for Akt1 versus control siRNA-transfected cells. *B*, BAEC transfected with control or Akt1 siRNA were stimulated with VEGF or S1P for the indicated times. Cells were lysed, and phosphorylation of AMPK, eNOS, and GSK3- β were analyzed in the cell lysates in immunoblots probed with phospho-specific antibodies as shown. Panel *C* shows densitometric analysis of pooled data, presenting the ratio between phosphorylated and total eNOS, phosphorylated and total AMPK, and phosphorylated and total GSK3- β in control and Akt1 siRNA-transfected cells, both under basal conditions and after treatment with VEGF and S1P for 5 min. Each data point represents the mean \pm S.E. derived from four independent experiments; the addition of VEGF and S1P induced a significant increase in phosphorylation of eNOS, GSK3- β , and AMPK in control siRNA-transfected cells ($p < 0.01$). *, $p < 0.05$; **, $p < 0.01$ for Akt1 versus control siRNA-transfected cells.

Fig. 7. Effects of AMPK siRNA on agonist-enhanced Rac1 activity. *A*, BAEC were transfected with control or AMPK α 1 siRNA and subsequently treated with S1P (100 nM) for 5 min or with VEGF (10 ng/mL) for 1 min; Rac1 activity in the cell lysates was measured by pull-down of GTP-Rac1 using the GST-p21-binding domain of PAK-1. Active and total Rac1 were detected in immunoblots using an anti-Rac1-specific antibody. Phospho-AMPK in the cell lysates was detected in immunoblots as shown. *B*, densitometric analysis of pooled data showing the ratio between active and total Rac1 after treatment with S1P and VEGF. Each data point represents the mean \pm S.E. derived from three independent experiments; the addition of S1P and VEGF induced a significant increase in Rac1 activity ($p < 0.01$). *, $p < 0.02$ versus S1P- or VEGF-treated control siRNA-transfected cells (*t*-test).

Fig. 8. Differential effects of Rac1 siRNA-mediated knockdown on phosphorylation of AMPK and the AMPK substrates ACC and eNOS. *A* shows the results of immunoblots analyzed in BAEC lysates prepared from cells transfected with control or Rac1 siRNA and treated with VEGF or S1P for the indicated times. Cell lysates were resolved by SDS-PAGE and probed using antibodies directed against phospho-AMPK, AMPK, phospho-ACC, ACC, phospho-eNOS, eNOS, and Rac1. Shown are the representative data of three independent experiments. *B* shows the results of densitometric analyses from pooled data, plotting the ratios of phosphorylated ACC and AMPK to total ACC and AMPK, respectively, relative to the signals present in the unstimulated control siRNA-transfected cells. Each data point represents the mean \pm S.E. derived from three independent experiments. *, $p < 0.05$ versus control siRNA-transfected cells (ANOVA).

Fig. 9. siRNA-mediated caveolin-1 knockdown enhances AMPK phosphorylation. *A*, BAEC were transfected with control or caveolin-1 siRNA; 48 h after transfection, cells were treated with VEGF (10 ng/ml) or S1P (100 nM) for the indicated times. Cell lysates were resolved by SDS-PAGE and analyzed in immunoblots probed with antibodies specific to the proteins or phosphoproteins as shown. Caveolin-1 expression was analyzed in immunoblots with anti-caveolin-1 antibody. Shown are the representative results of an experiment that was repeated three times with equivalent results. *B*, pooled data from time course experiments in which the relative intensity of each data point in VEGF- and S1P-treated cells was analyzed by densitometry. Each point in the graph represents the mean \pm S.E. of three independent experiments. *C*, the results of densitometric analyses showing the ratios of phospho-AMPK to total AMPK and phospho-GSK3- β to total GSK3- β in caveolin-1 siRNA or control siRNA-transfected

cells in basal conditions and after treatment with VEGF or S1P for 2 min. Each data point represents the mean \pm S.E. derived from three independent experiments. The addition of either VEGF or S1P induced a significant increase in phosphorylation of AMPK ($p < 0.005$). *, $p < 0.001$ for caveolin-1 versus control siRNA transfected cells (ANOVA).

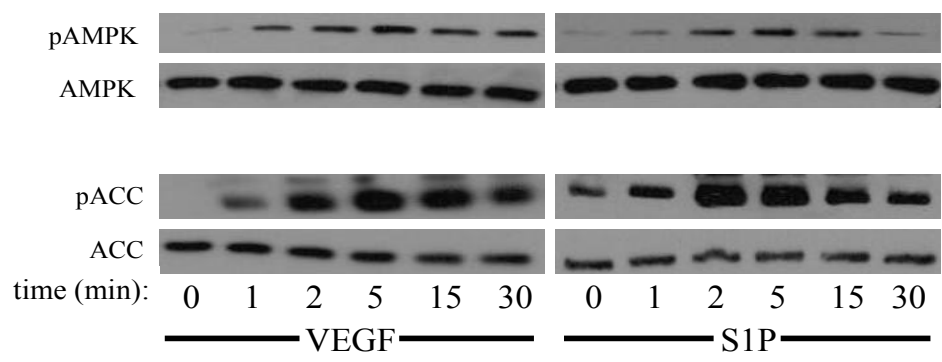
Fig. 10. siRNA-mediated knockdown of AMPK and its substrates impairs VEGF- and S1P-induced endothelial cell migration. Endothelial cell migration was measured using a Transwell system in BAEC transfected with duplex siRNA targeting constructs for AMPK, Rac1, Akt1, or eNOS or with control siRNA. In *A*, one well from a 6-well plate was set aside for each condition, and cell lysates were prepared, resolved by SDS-PAGE, and immunoblotted using AMPK, Rac1, Akt1, and eNOS antibodies as shown. Panel *B* shows the results of a cell migration assay analyzing the migration of siRNA-transfected cells treated with VEGF (10 ng/mL) or S1P (100 nM), as described in “Experimental Procedures.” The panel shows pooled data of migrated cells, presenting as the *migration index*, which represents the number of migratory cells following siRNA transfection/number of migratory cells determined under basal conditions in control siRNA-transfected BAEC. For all cells, the addition of VEGF or S1P induced a significant increase in endothelial cell migration ($p < 0.05$). *, $p < 0.05$ versus corresponding treatment in control siRNA-transfected cells (using ANOVA).

Fig. 11. AMPK-dependent endothelial tube formation. BAEC were transfected with control, caveolin-1, AMPK, Rac1, or eNOS siRNA; 48 h after transfection, the cells were trypsinized and resuspended in FBS-supplemented media, and 3×10^4 cells were plated into each well of a 24-well plate coated with Matrigel. The tubes were photographed and analyzed by a blinded observer 9 h after plating. *A* shows representative images of endothelial tube formation by BAEC transfected with control siRNA (1), AMPK siRNA (2), Rac1 siRNA (3), and eNOS siRNA (4). *B*, The average total tube length (TTL) per field of view (FOV) is shown with SEM derived from 9 independent experiments. * indicates a statistically significant difference ($p < 0.02$) compared to the TTL per FOV of BAEC transfected with control siRNA. *C*, Individual tube length (in number of pixels) is grouped into 9 categories: 1 (0-49), 2 (50-99), 3 (100-149), 4 (150-199), 5 (200-249), 6 (250-299), 7 (300-349), and 8 (350-399).

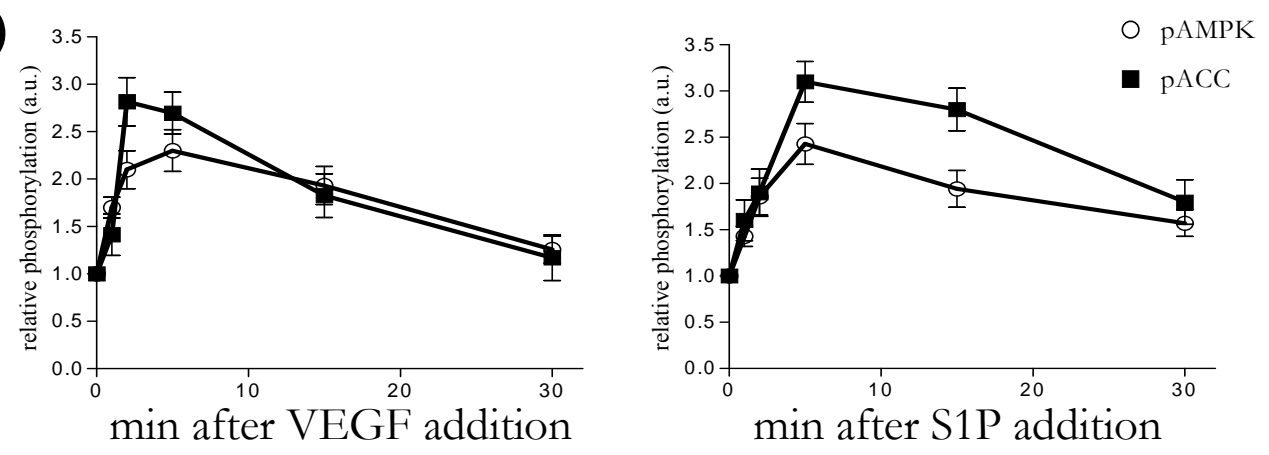
Fig. 12. Scheme for VEGF- and S1P-mediated regulation of AMPK in BAEC. In this model, VEGF and S1P differentially phosphorylate AMPK, which can then activate Rac1. Rac1 activation, in turn, is required for the activation of PI3K, which then, via PDKs, activates Akt. Akt then phosphorylates GSK3- β and eNOS. Caveolin-1 acts as a negative regulator of AMPK. Rac1 also modulates AMPK-mediated ACC phosphorylation. Please see text for details.

Fig.1

A)



B)



C)

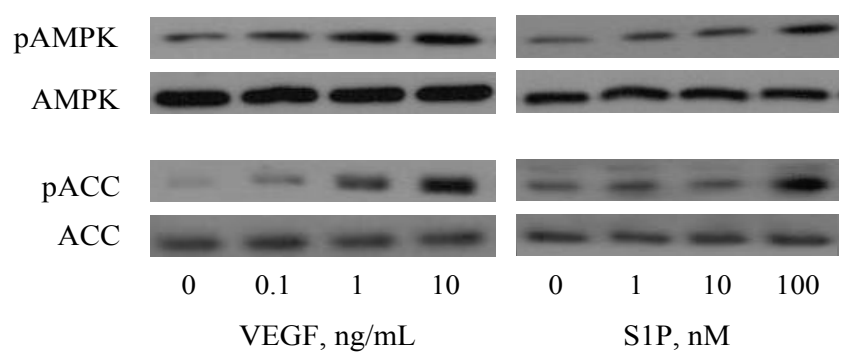
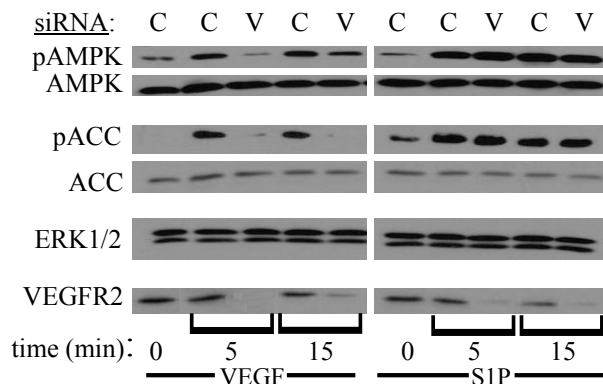
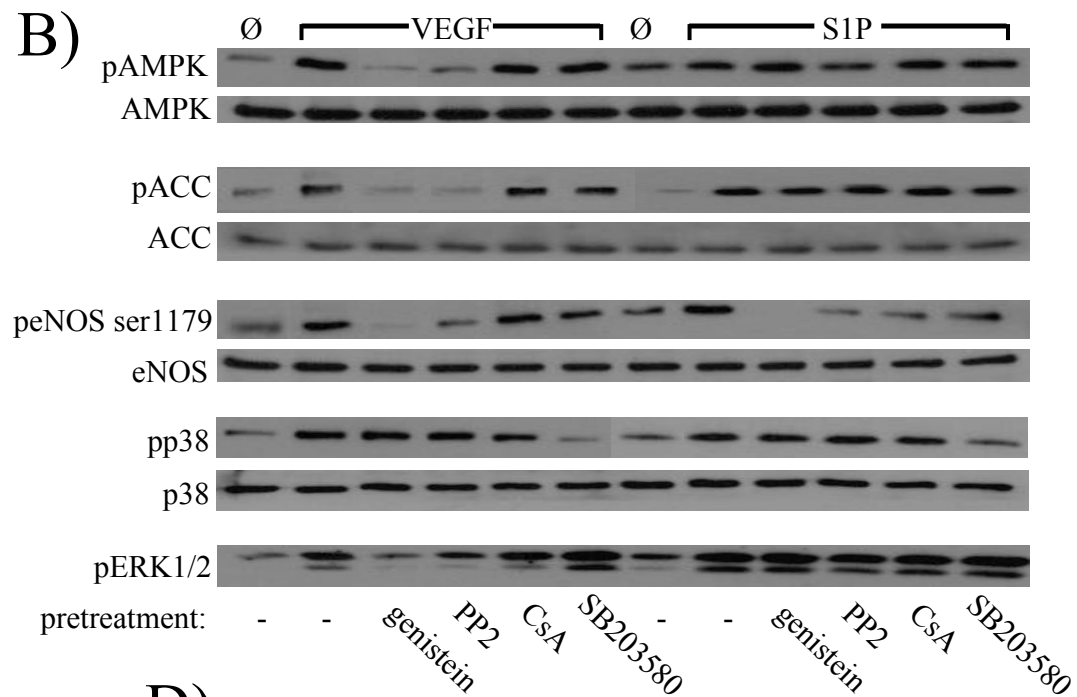


Fig.2

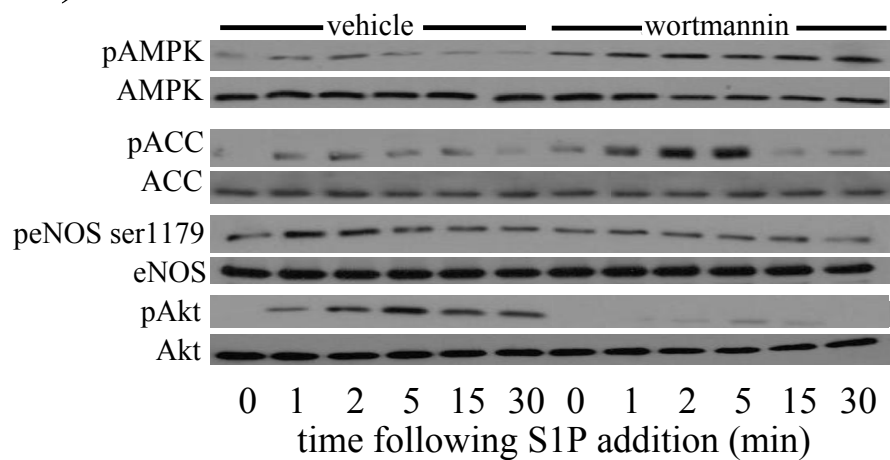
A)



B)



C)



D)

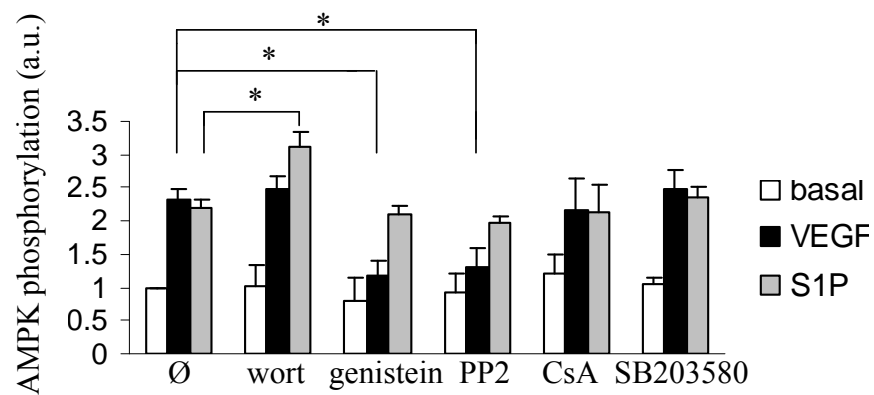
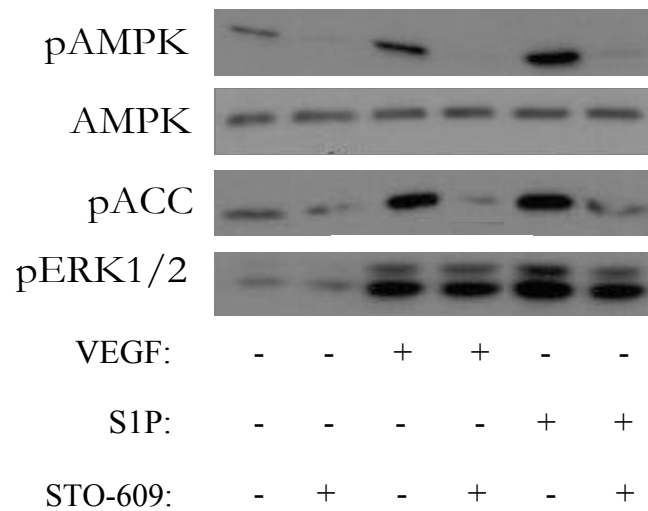


Fig.3

A)



B)

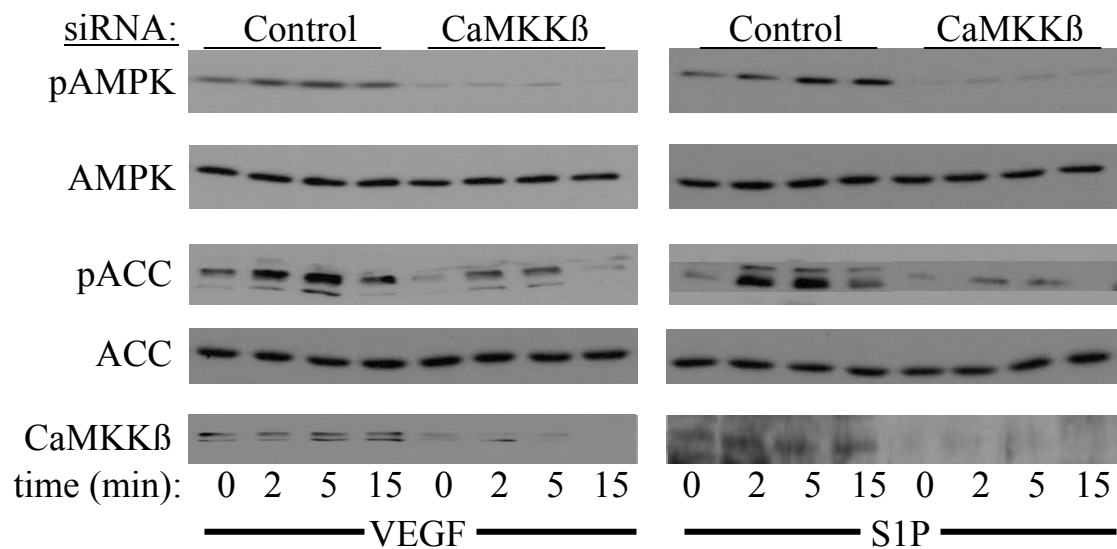
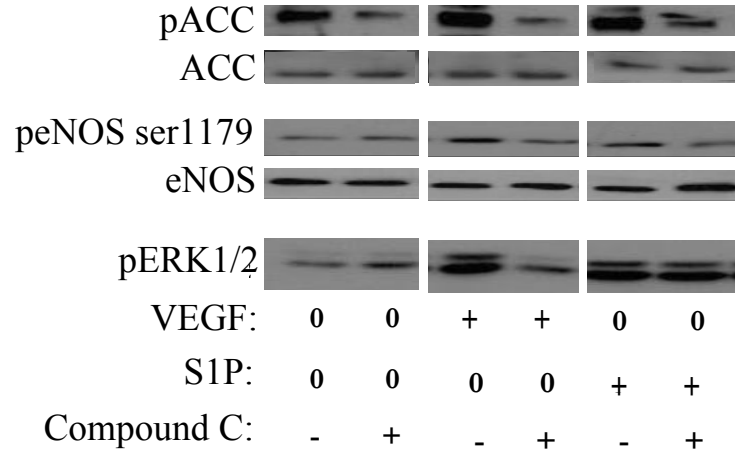
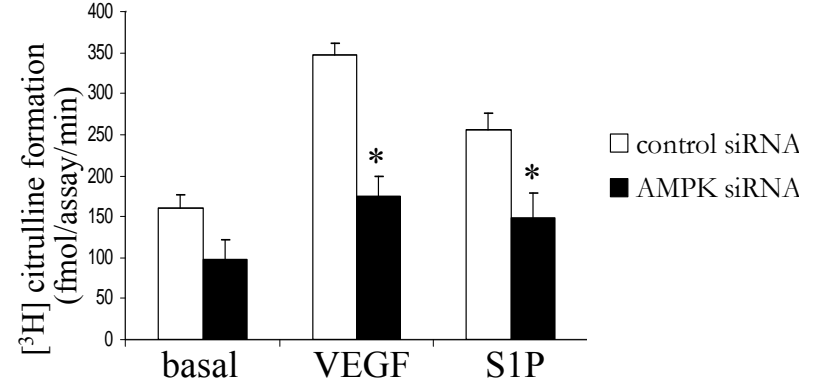


Fig.4

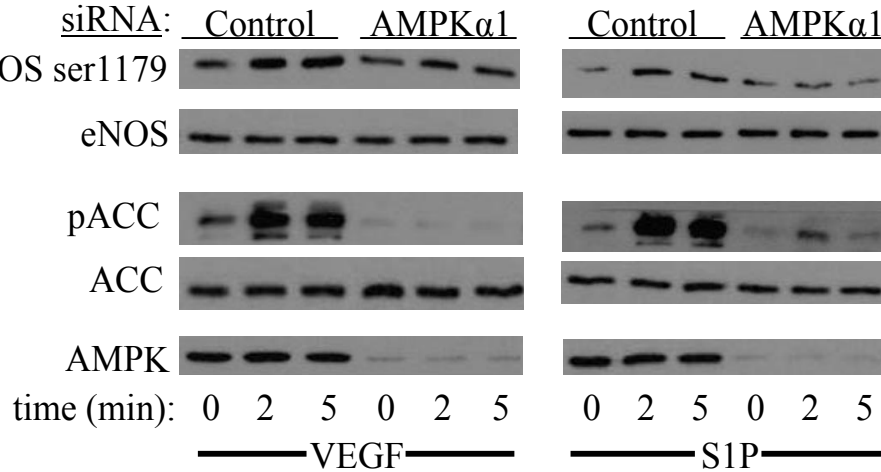
A)



B)



C)



D)

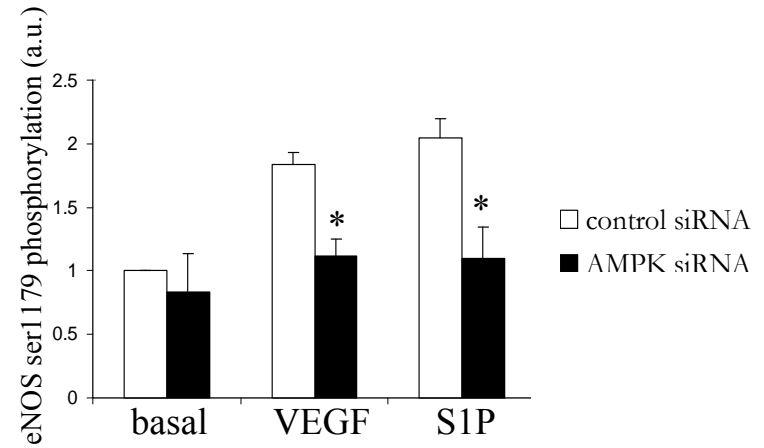
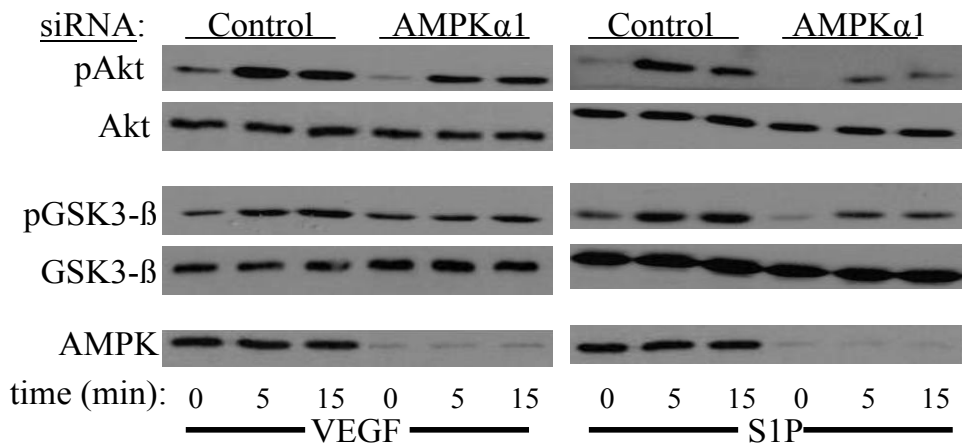


Fig.5

A)



B)

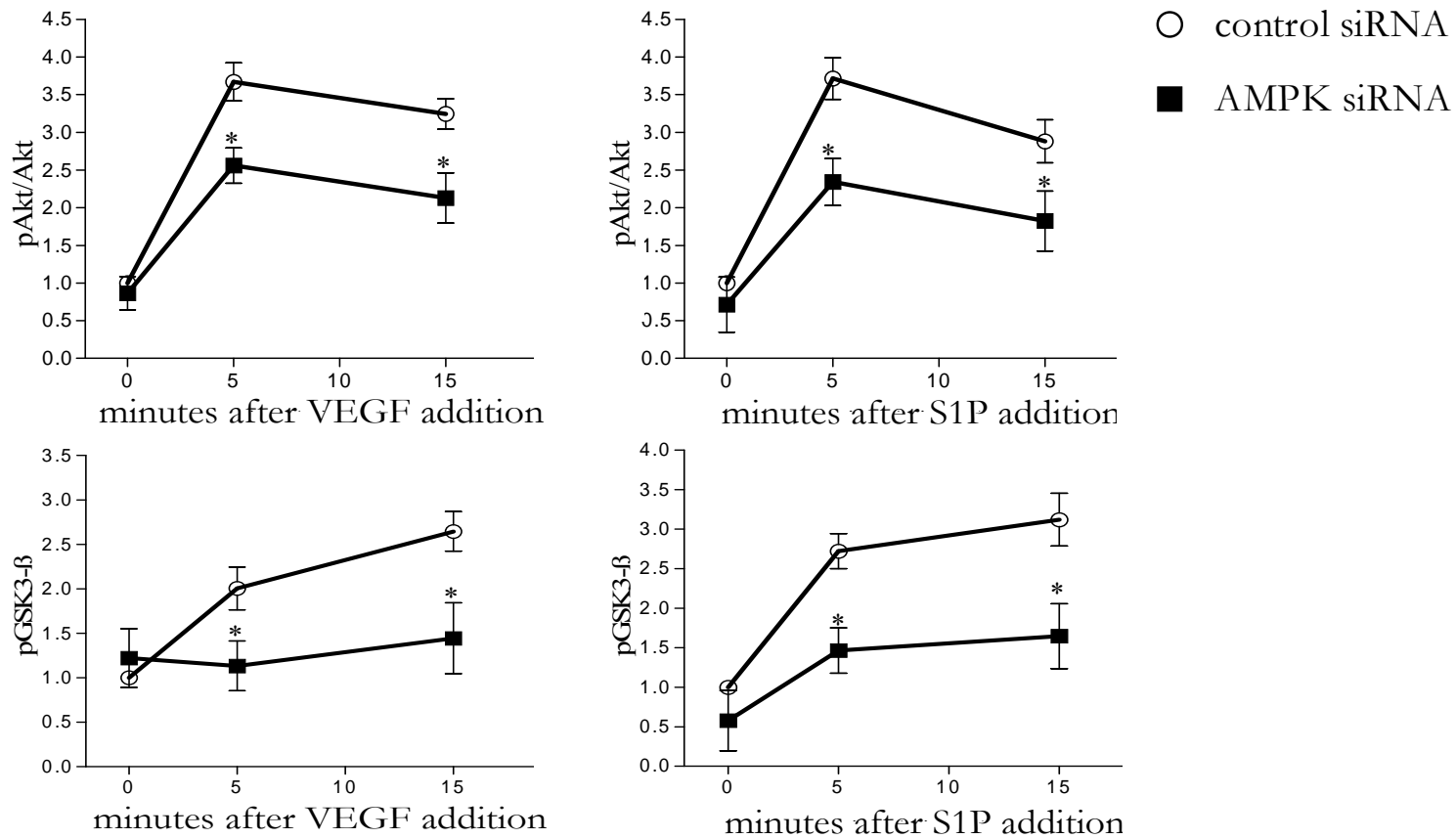
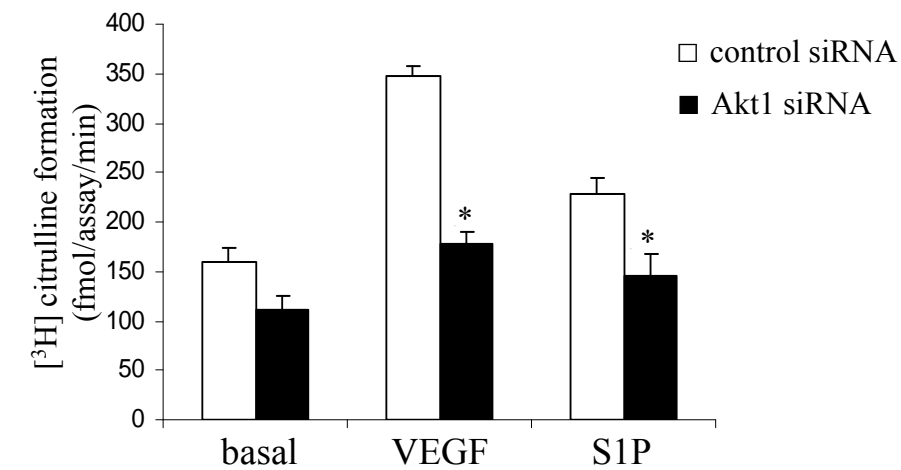
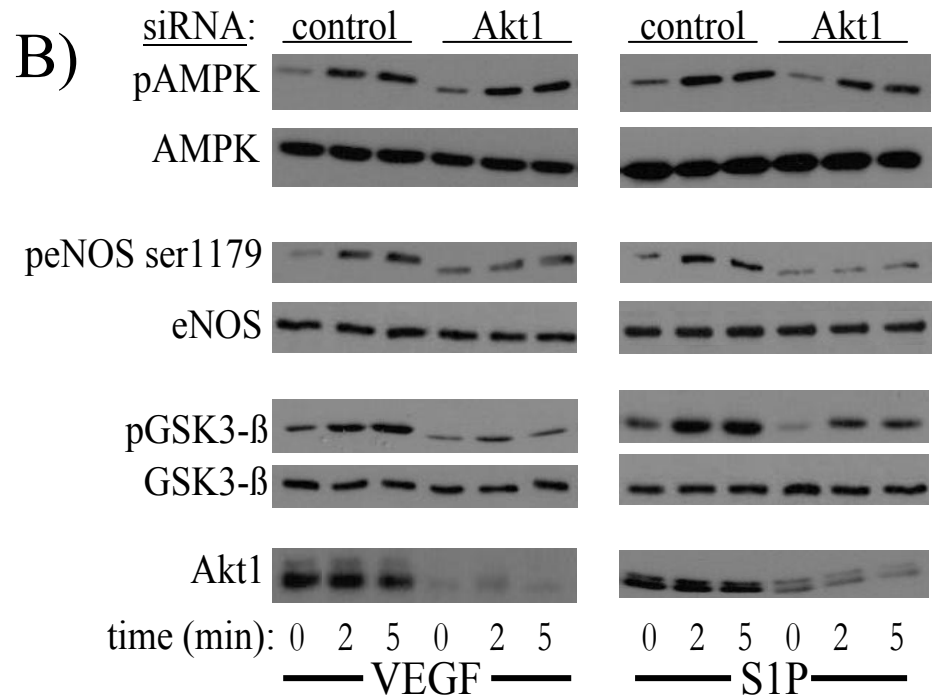


Fig.6

A)



B)



C)

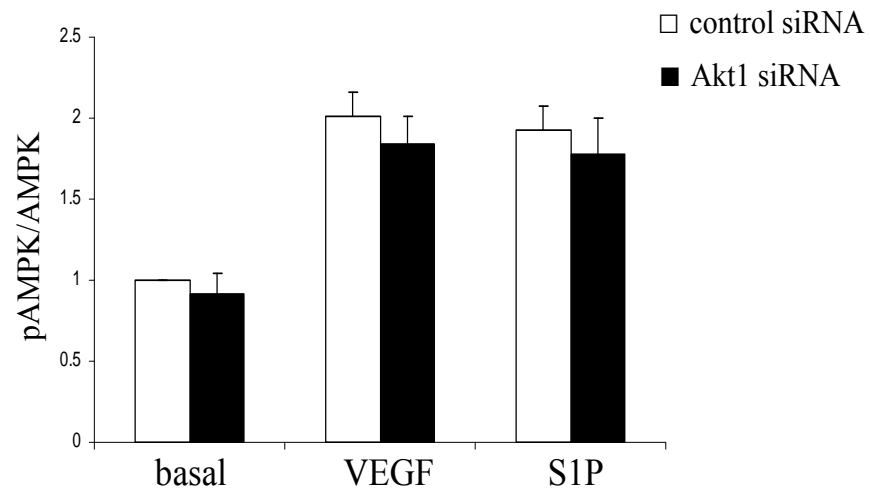
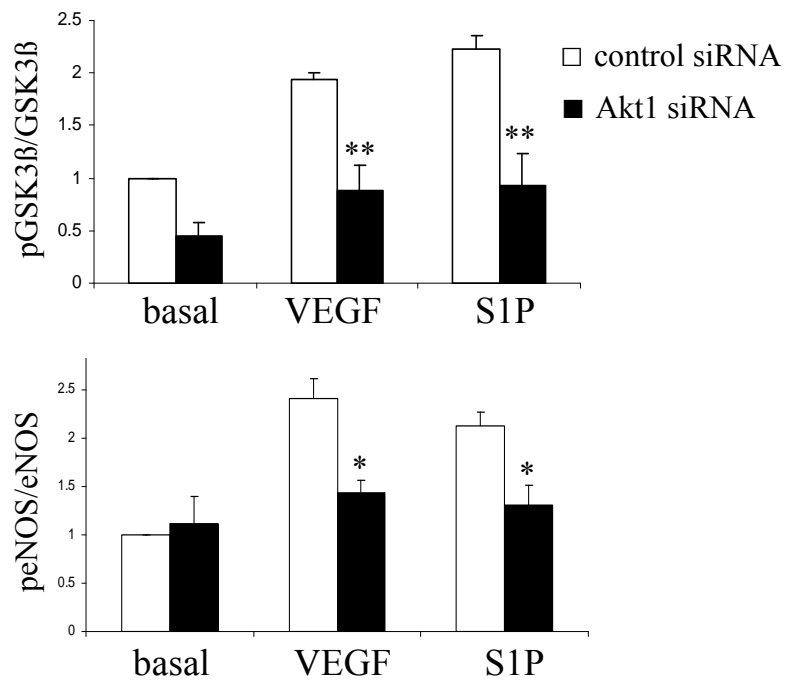
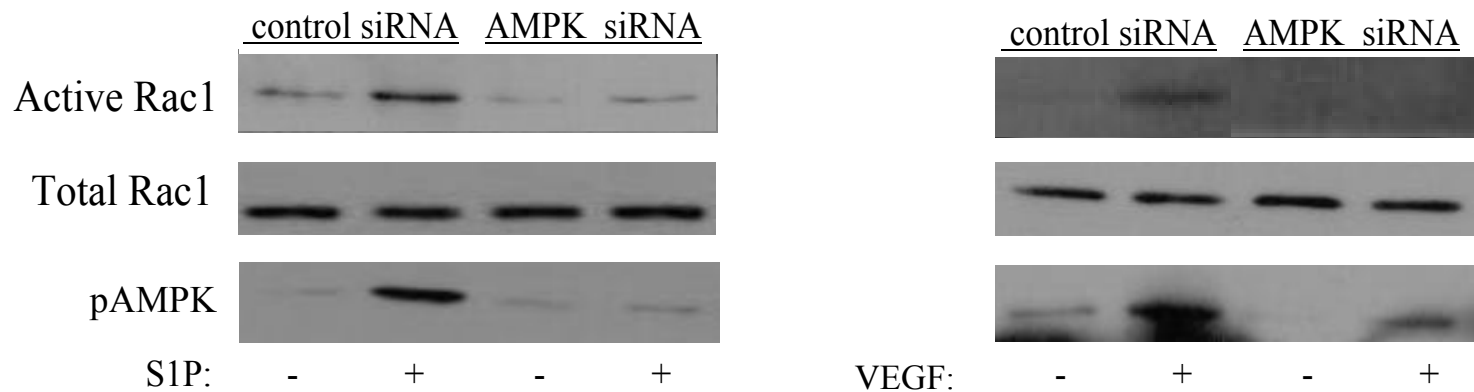


Fig.7

A)



B)

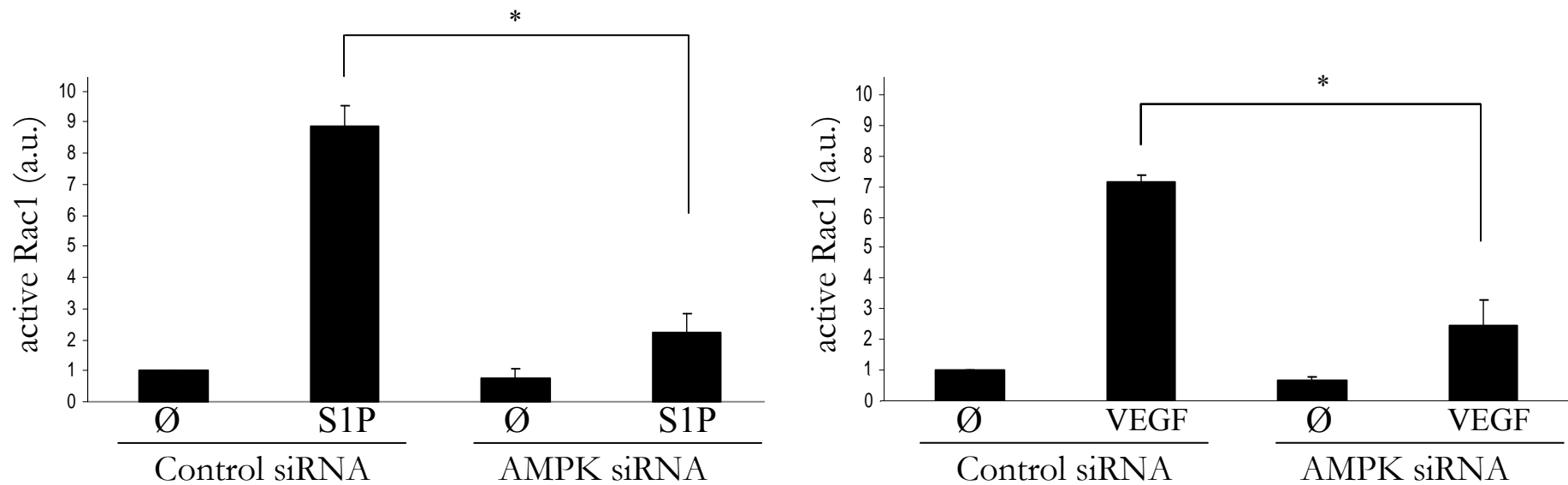
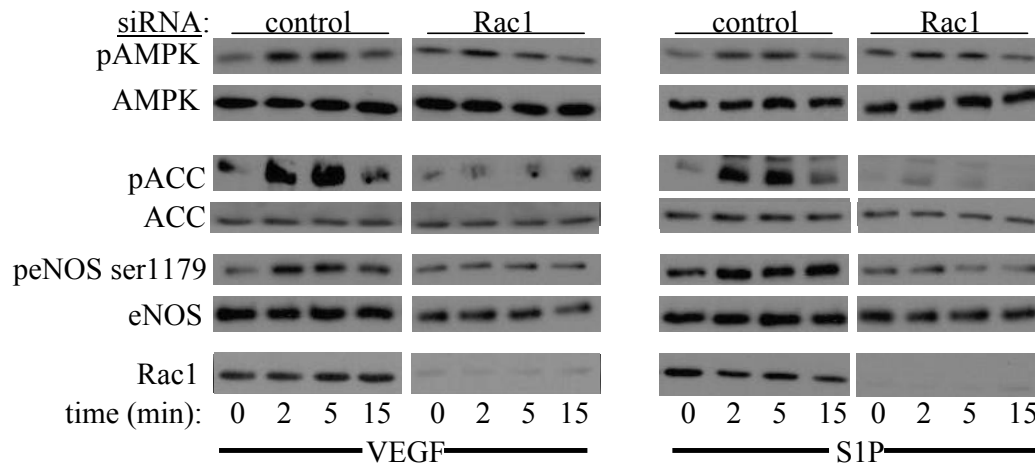


Fig.8

A)



B)

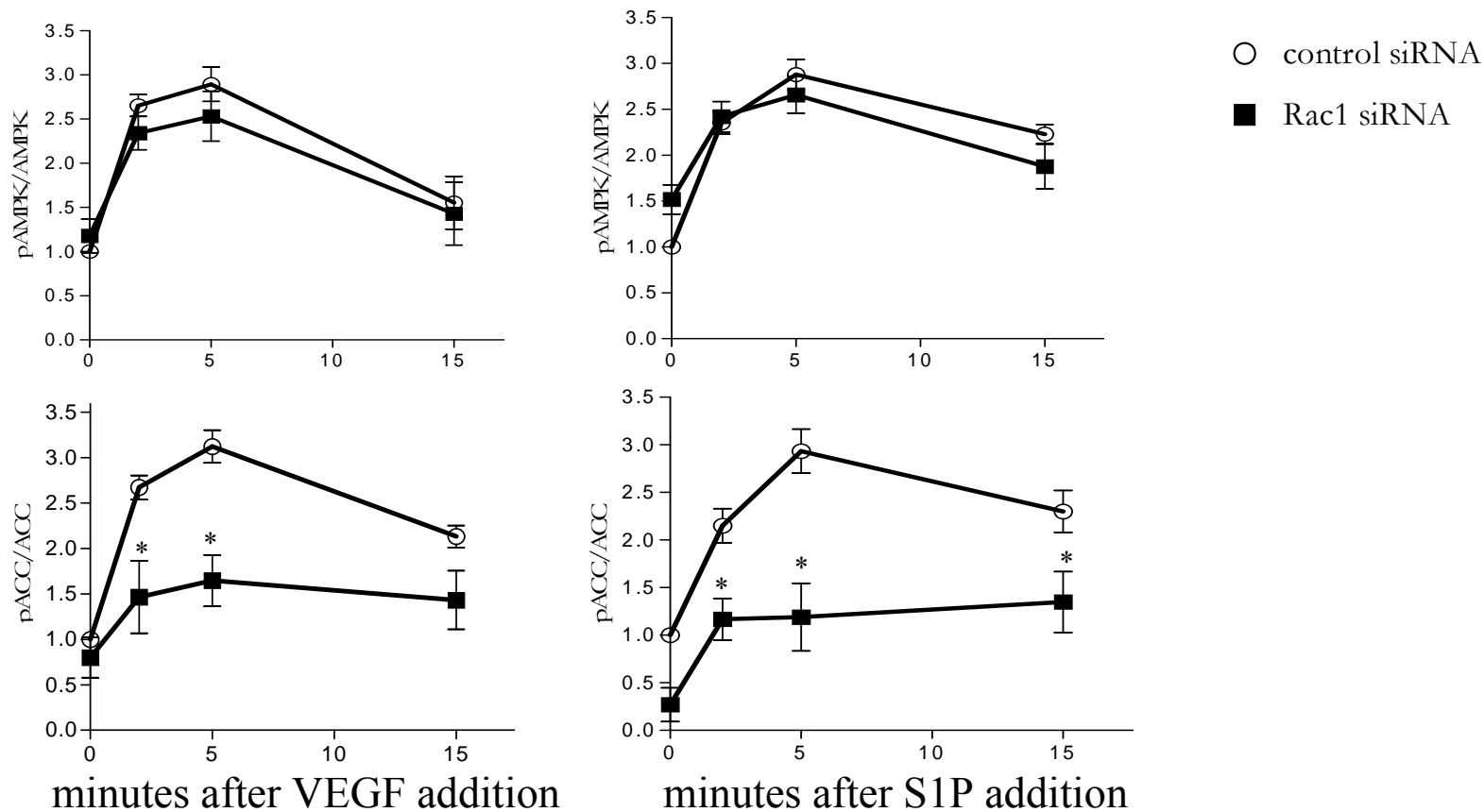
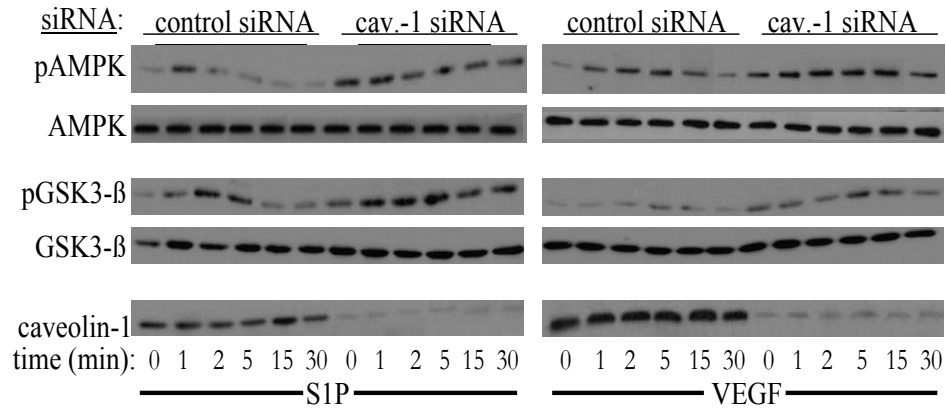
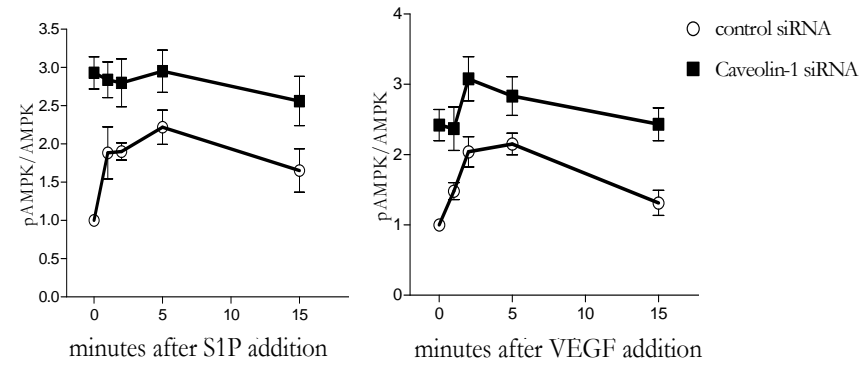


Fig.9

A)



B)



C)

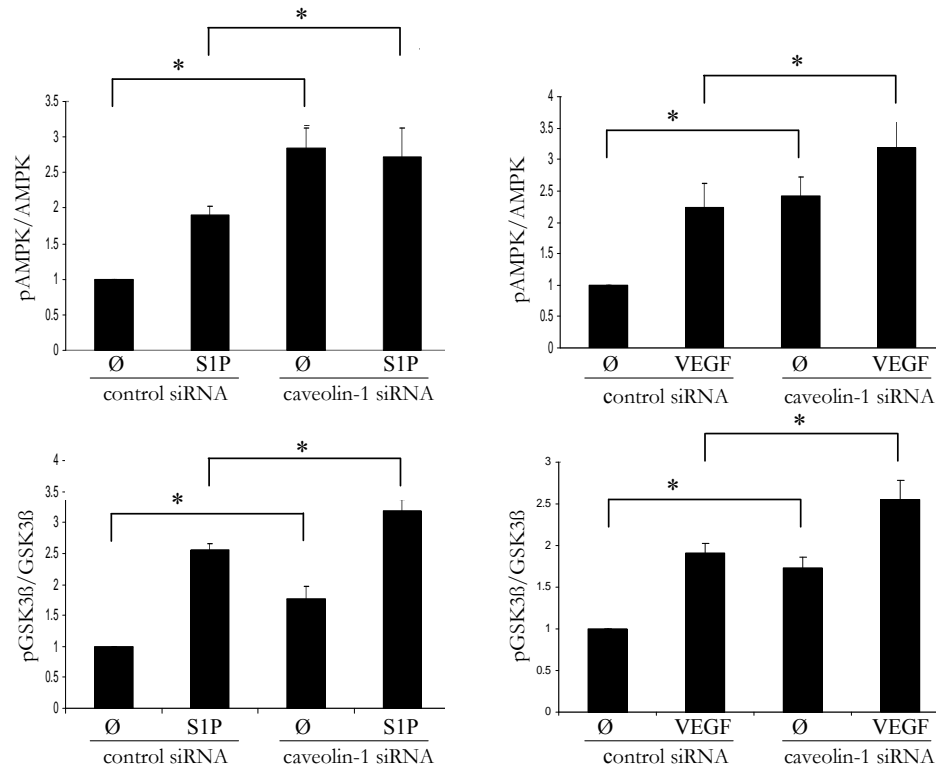


Fig.10

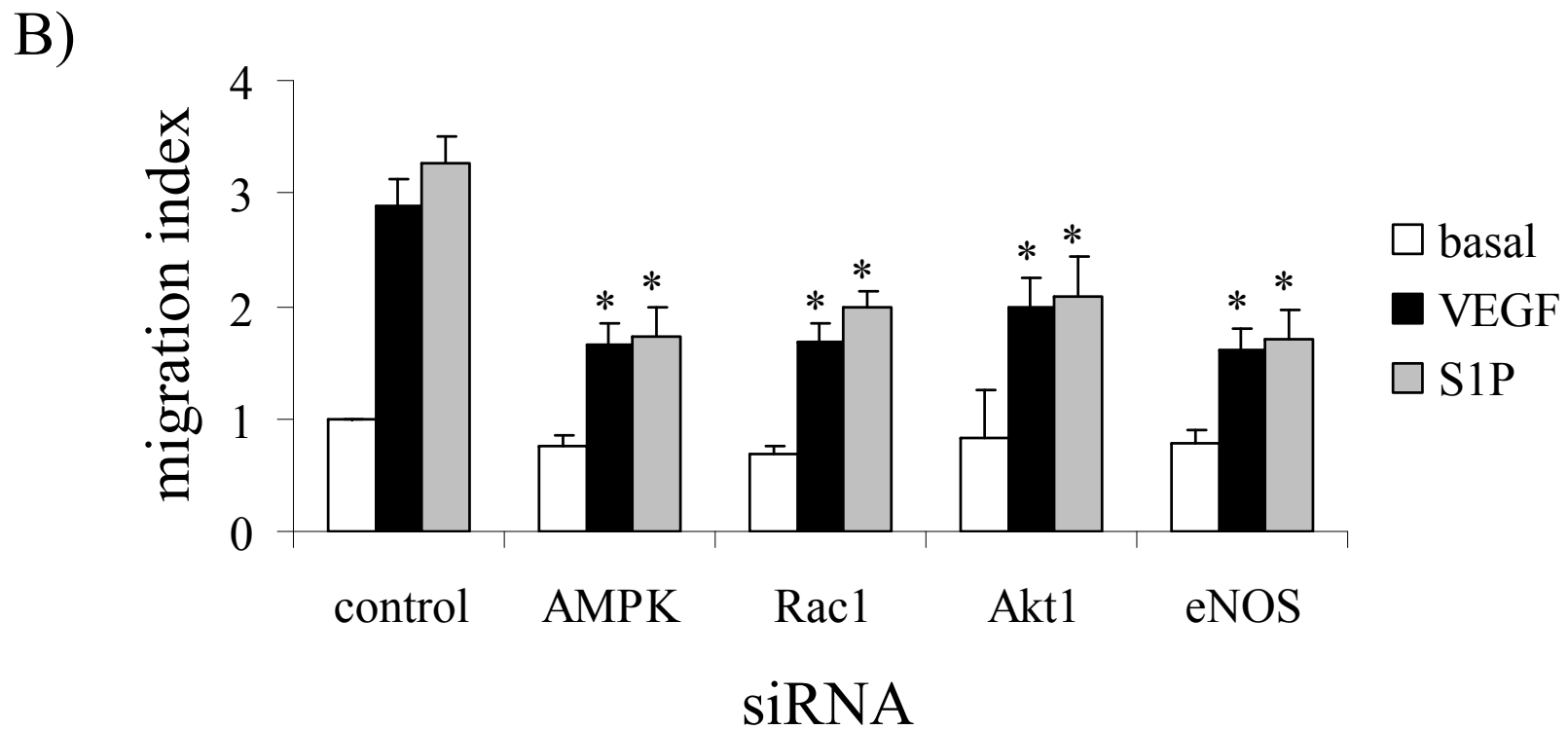
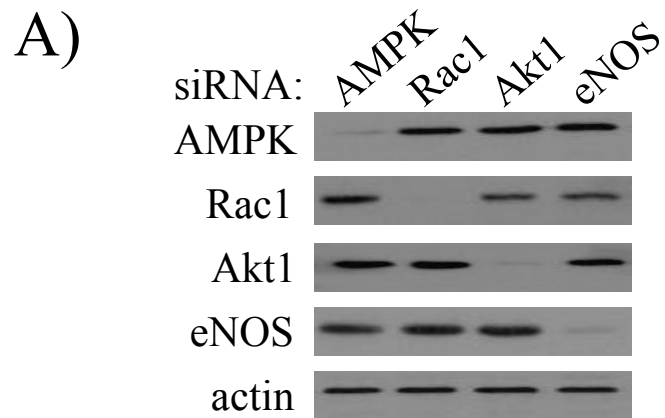


Fig.11

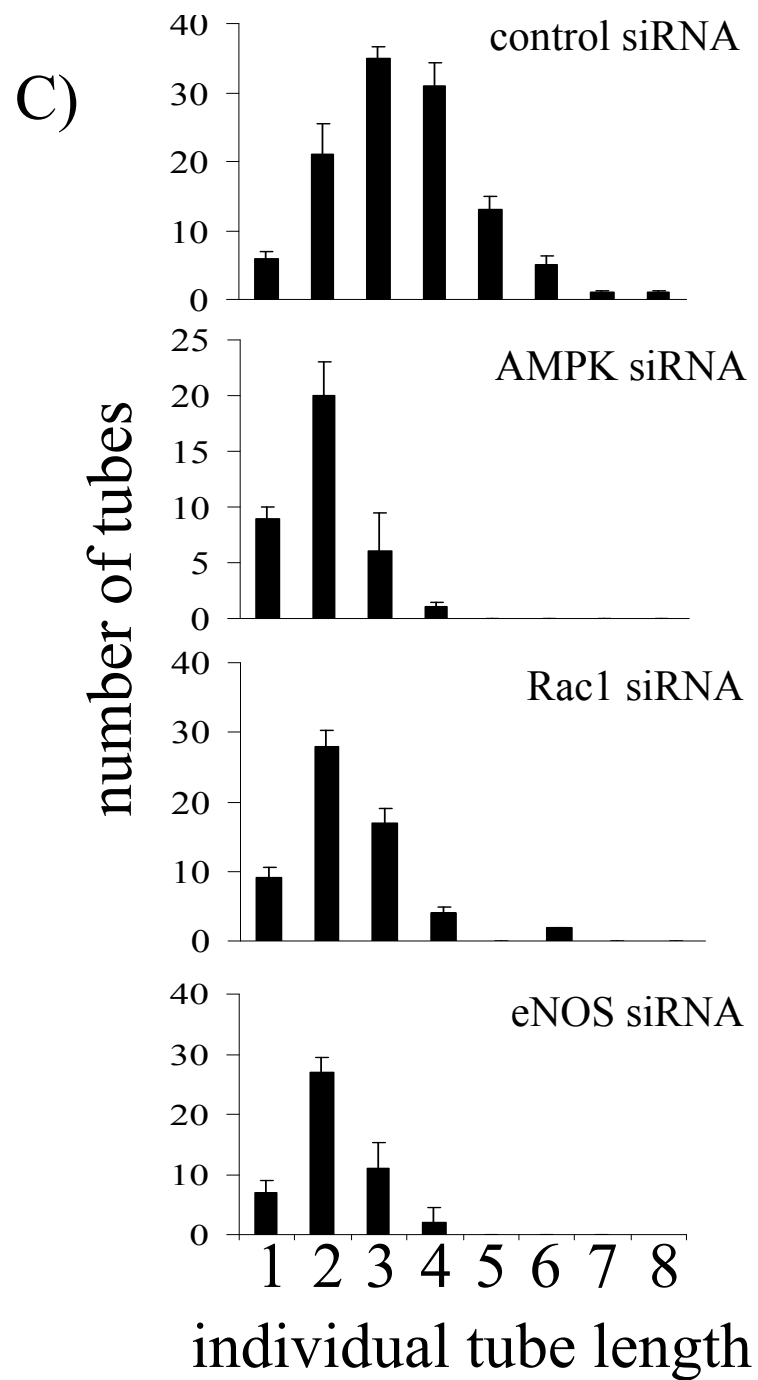
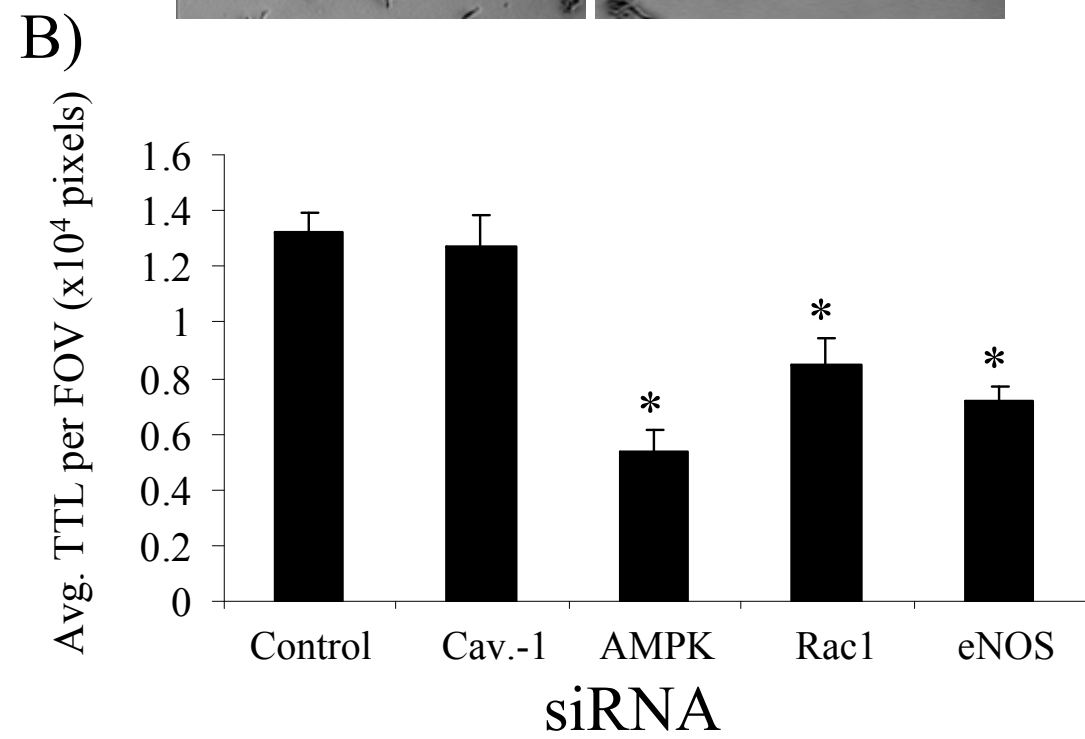
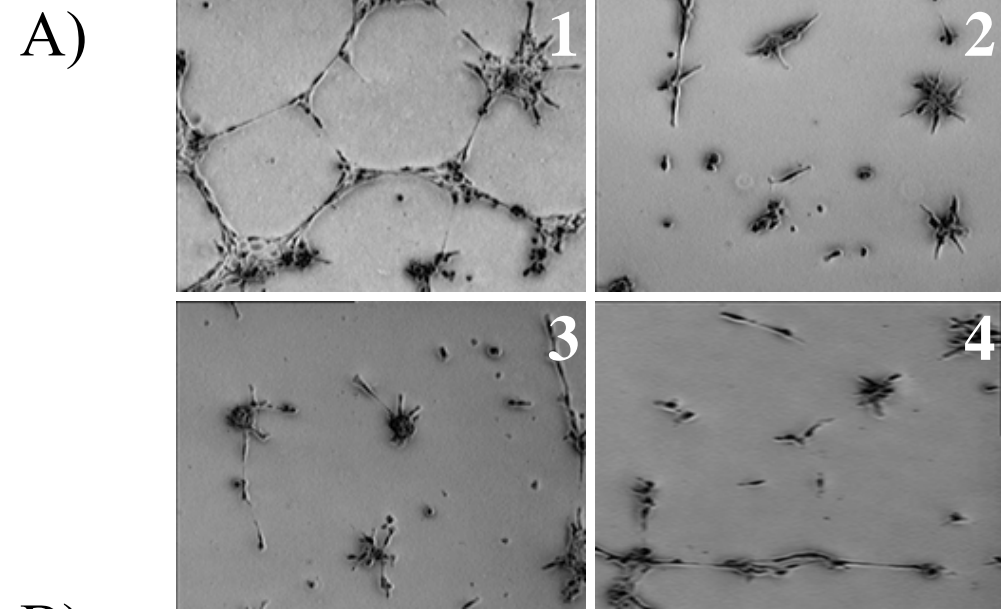


Fig.12

